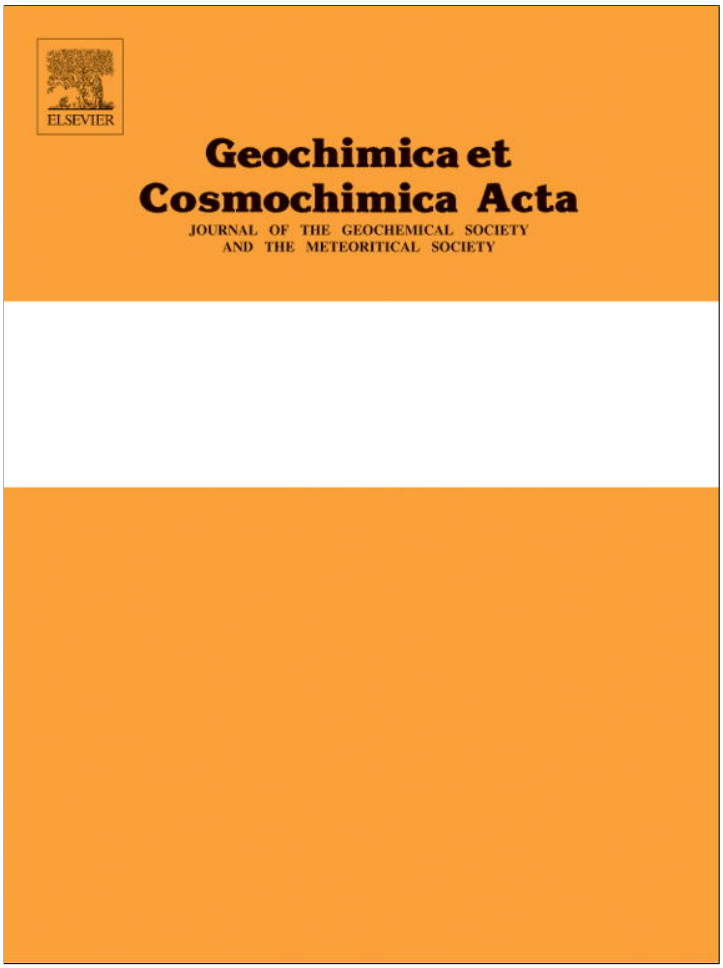


(This is a sample cover image for this issue. The actual cover is not yet available at this time.)

Available online at www.sciencedirect.com

SciVerse ScienceDirect

Geochimica et Cosmochimica Acta 104 (2013) 63–83

Geochimica et Cosmochimica Acta

www.elsevier.com/locate/gca

# Mineralogy and geochemistry of the Mahi River sediments in tectonically active western India: Implications for Deccan large igneous province source, weathering and mobility of elements in a semi-arid climate

Anupam Sharma [a,*], Sarajit Sensarma [b], Kamlesh Kumar [c], P.P. Khanna [d], N.K. Saini [d]

[a] Central University of Himachal Pradesh, P.O. Box 21, Dharamshala 176 215, India
[b] Centre of Advanced Study in Geology, University of Lucknow, Lucknow 226 007, India
[c] Birbal Sahni Institute of Palaeobotany, 53 University Road, Lucknow 226 007, India
[d] Wadia Institute of Himalayan Geology, 33 General Mahadeo Singh Marg, Dehradun 248 001, India

Received 28 March 2012; accepted in revised form 2 November 2012; Available online 3 December 2012

**Abstract**

Large igneous provinces (LIPs) hosting mafic rocks over million km$^2$ are likely to influence global sediment production and distribution and help in resolving discrepancies in upper continental crust (UCC) compositions. This work focuses on the texture, mineralogy, and compositions including REE of fine sand/silt deposited by a small to medium-sized river, the Mahi River (about 600 km) in a tectonically active, semi-arid region draining the Deccan Traps in western India, one of the largest LIPs in the world. The results are also applied to a sedimentary rock of fluvial origin (Siwalik mudstone/siltstone) to ascertain the source characteristics of this alluvium and evaluate comparative element (K, Ba, Sr, Na, Ca and Mg) mobility.

The Mahi sediments are lithiarenite, mostly composed of quartz and basalt fragments with lesser pyroxene, biotite, feldspar, calcite and clay minerals (smectite ± illite). The Mahi sediments have higher FeO′ ($\leqslant$10.9 wt.%), $TiO_2$ ($\leqslant$2.41 wt.%), $Al_2O_3$ ($\leqslant$15.2 wt.%), Cr ($\leqslant$737 ppm), Co ($\leqslant$36 ppm), Cu ($\leqslant$107 ppm) than the UCC and PAAS; Ni ($\leqslant$54 ppm) higher than the UCC (33.5 ppm), but similar to PAAS (60 ppm). The low CIA (37–59) values and presence of basalt fragments and smectite in the samples suggest incipient weathering in the semi-arid Mahi catchment. In agreement with the mineralogy, the UCC-normalized LREE depleted patterns (LREE/HREE < 1) in the Mahi sediments confirm Deccan basalt contributions from the provenance with about 70–75% basalts and 25–30% Archean biotite-rich granitoids. The mafic contribution, in addition to the UCC, is important for the Siwalik rocks too.

Similarly limited depletion of Ba, K and Ca (Ba $\geqslant$ K > Ca) in weathering-limited Mahi (aver CIA 47.5) and transport-limited Siwalik (aver CIA 69) systems indicate their climate insensitivity. At the same time, more Ba depletion than Ca is new for the Deccan Traps River. Decoupling of Ca and Sr, however, could be mineralogy controlled.


## 1. INTRODUCTION

Rock weathering and erosion are two fundamental earth surface processes intrinsic to sediment formation and element distribution (e.g., Suttner, 1974; Stallard and Edmond, 1983; Basu, 1985; Sharma and Rajamani, 2001; Singh and Rajamani, 2001). The composition of the upper

* Corresponding author. Address: School of Earth and Environmental Sciences, Central University of Himachal Pradesh, P.O. Box 21, Dharamshala, Himachal Pradesh 176 215, India. Tel.: +91 01892 229330; fax: +91 01892 237286.
*E-mail address:* anupam110367@yahoo.com (A. Sharma).

0016-7037/$ - see front matter © 2012 Elsevier Ltd. All rights reserved.
http://dx.doi.org/10.1016/j.gca.2012.11.004

continental crust (UCC) is approximately granodioritic ($SiO_2$ 55–66 wt.%), typically forming at the present-day convergent margins (Taylor and McLennan, 1985). During fluvial reworking, sediments get homogenized and effectively represent average 'granodioritic' continental crustal compositions (Taylor and McLennan, 1985; Rudnick and Gao, 2003). However, there are discrepancies regarding the concentrations of certain trace elements. For example, discrepancies in Cr and Co concentrations by nearly a factor of 2–3 seem common (McLennan, 2001). Weathering accounts for ~20% Mg loss from the continents, aiding in the formation and sustenance of a Si-rich and Mg-poor continental crust (Lee et al., 2008), in addition to granodiorite production through magmatic processes. The La/Nb ratio in the continental crust is better modeled by mixing between intraplate basalt and convergent margin magmas (Rudnick, 1995). Thus the global continental provenance may not necessarily be of granodiorite compositions only, but it could have a more mafic component.

Mafic to ultramafic igneous rocks have higher contents of Cr, Co, Cu than silicic and intermediate igneous rocks (Brügmann et al., 1987). The large igneous provinces (LIPs) (e.g., continental flood basalt provinces) host significant amounts of mafic rocks on the Earth's surface, covering about $50–100 \times 10^3$ km$^2$ (e.g., Sensarma, 2007; Sheth, 2007; Bryan and Ernst, 2007). Altogether somewhat more than 150 LIPs are known (see Bryan and Ernst, 2007) and the number of LIPs is expanding with better identification and recognition throughout the geologic record. This makes LIPs to stand out as an important provenance worth considering in the models of continental crustal composition and its evolution. The origin of LIPs is a major area of research in understanding global mantle and crust/mantle systems (http://www.largeigneousprovince.org; http://www.mantleplume.org). The possible role of LIPs, with the abundant presence of more weatherable mafic rocks, in sediment production and global sediment supply is not adequately known. This is important because LIPs may have significant contributions in influencing the upper crustal compositions and help to address discrepancies of the elemental abundances mentioned above.

The Himalayas and the Deccan LIP are the two most important geologic entities of global significance in India. The contributions of the Himalayan lithology, tectonics, and climate in sediment production and distributions are well recognized (e.g., Sarin et al., 1989; Krishnaswami et al., 1992; France-Lanord and Derry, 1997; Gaillardet et al., 1999; Galy and France-Lanord, 2001; Singh et al., 2006, 2008). Limited research, however, has been done on the role of the Deccan LIP on this aspect, though it covers ~0.5% of the global drainage area (Das and Krishnaswami, 2006).

The mainland Gujarat region in western India has several rivers including the Tapti and Narmada that flow from the Peninsular India into the Arabian Sea (Fig. 1a and b) passing through the Deccan Province and they must have been carrying sediments from multiple sources, including the Deccan basalts. Except for some geochemical study of dissolved load of the rivers draining the Deccan province (e.g., Dessert et al., 2001, 2003; Gupta and Chakrapani, 2005, 2007; Das et al., 2005; Das and Krishnaswami, 2007; Sharma and Subramanian, 2008; Gupta et al., 2011), limited mineralogical and geochemical study of these sediments have been done. Moreover, these rivers are relatively small (<~600 km), carry higher ionic load (Sharma et al., 2012), and are thus good candidates for unraveling weathering processes, sediment production and distribution, and their source rock characteristics.

As part of our ongoing research on western Indian fluvial sediments, comparison between the Mahi River sediments and the surrounding rocks from which they were derived allows us to better explore the link between the sedimentary record and the large Deccan basaltic provenance. In this paper, we discuss the mineralogy and geochemistry of a ~8.5 m thick deposit exposed near Mujpur village (22°09′07″N: 72°35′28″E) in the lower Mahi River Basin. Textural and mineralogical data of sediments, bulk major element, and trace element compositions are combined to develop an integrated model to understand the relative control of tectonic–climate–lithology and source area characteristics for the Mahi sediments. Finally, the results are applied to the alluvium in the sedimentary rock of the Siwalik mudstone/siltstone to test its source characteristics and evaluate mobility of certain elements. This study has an important bearing on the general understanding of the role of LIPs in the petrogenesis of clastic sediment production and composition.

## 2. STUDY AREA AND PREVIOUS WORK

The Mahi River, approximately 600 km long, emerges near the Sardarpur District (Madhya Pradesh) and starts flowing North-Westerly to enter into the southern Rajasthan where it takes a southwesterly turn. The river then flows along the intercontinental Cambay Graben (Biswas, 1987) to meet the Cambay Bay (Fig. 2). The intersection of Precambrian orogenic trends, the NE–SW Aravalli trend, and the ENE–WSW Satpura trend/Narmada-Son lineament (NSGF) led to formation of several rift basins (e.g., Narmada, Cambay and Kutch rift basins) (Biswas, 1987) (Fig. 1c). The Bhuj Earthquake (intensity 6.9 on Richter scale) in 2001 suggests tectonic activity in the terrain continues to the present-day. The Mahi River largely flows in the upper reaches over the Deccan Traps (basalts, picritic basalts, minor rhyolite), sedimentary-metasedimentary rocks of the middle Proterozoic Vindhyan Supergroup, the 2.5 Ga Aravalli Supergroup rocks (leucogranite intrusions, metasediments, granites, minor komatiites, amphibolites) and the still older 3.5 Ga banded gneissic complex (BGC) rocks (Fig. 2). The BGC is predominantly composed of biotite granite gneiss with enclaves and inclusions of amphibolites (komatiitic), quartzite and calcareous rocks, and minor pegmatite.

A complex interplay of tectonism, climate and base level changes during the Holocene were responsible for sedimentation in the area by marine, fluvio–marine, fluvial and possibly some aeolian processes (e.g., Chamyal et al., 2003 and references therein; Tandon et al., 1999; Rachna et al., 1999; Maurya et al., 2000; Juyal et al., 2006; this work). The Middle Holocene Mujpur succession represents tidal estuarine

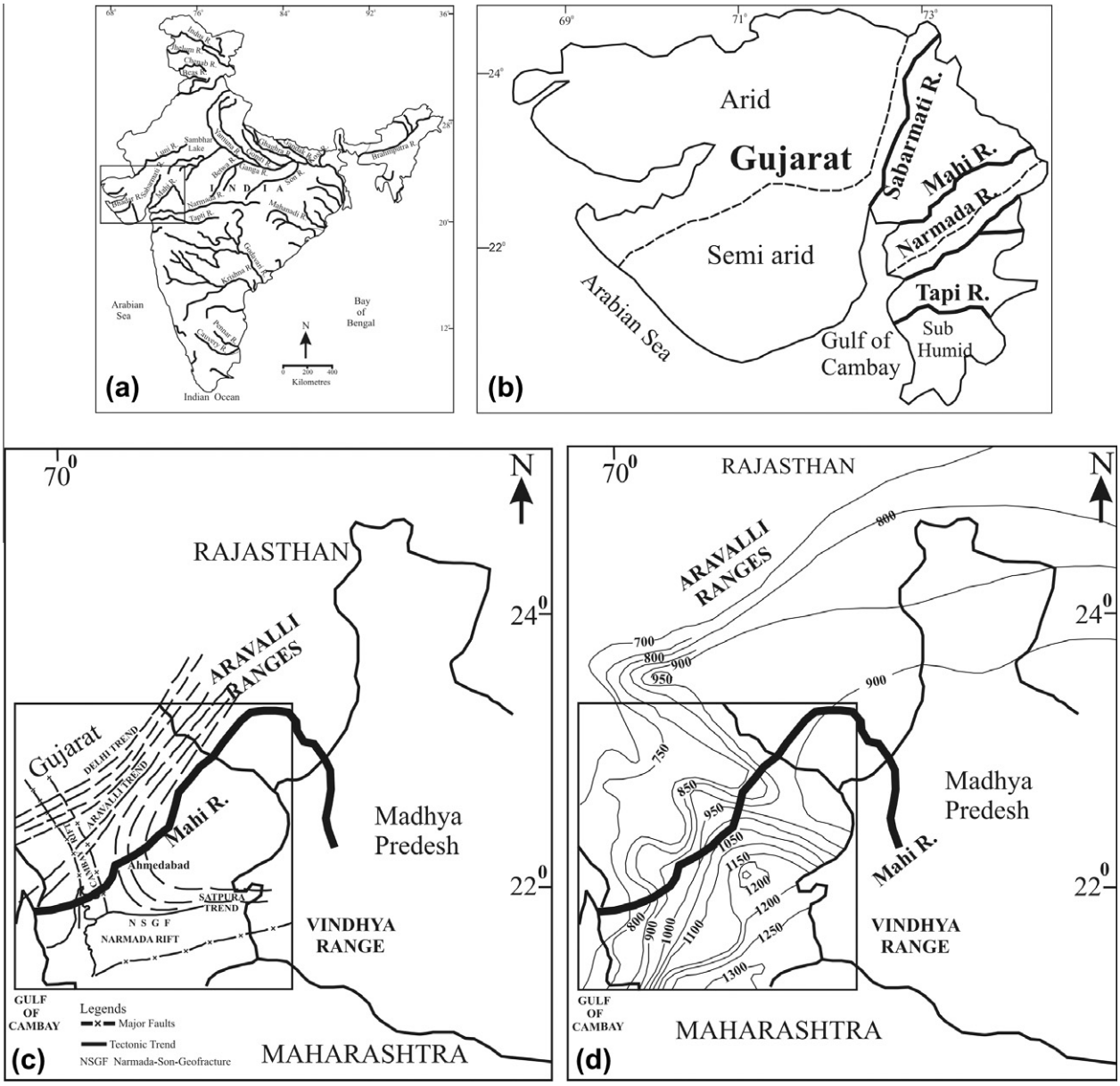


Fig. 1. (a) Map of India showing major rivers, mostly flowing easterly to south-easterly. Rivers in central-western India, however, flow westerly. Study area in inset. (b) Important rivers in the state of Gujarat (western India) including the Mahi river, (c) intersection of NE–SW and E–W tectonic trends in the Mahi river catchments (after Merh, 1995), and (d) annual rainfall distribution pattern (isohyets contour in mm) in the Mahi catchments. Data from Merh (1995).

deposits having mud-sand-silt intercalations (transitional environment) with successively coarser, fluvial sands (Kusumgar et al., 1998). Sedimentary structures (e.g., cross-bedding and ripple marks) are common; fine laminae are more common in the lower part and contain marine micro-fauna. In the light of the interpretation for the ~2.5 Ga finer mud-dominated succession that coarsens upward as of transitional environment (Chakraborty and Sensarma, 2008) and presence of marine micro-fauna in the Mahi samples suggest fluvial/fluvio–marine condition of deposition for the Mujpur section.

The general climate varies from sub-humid to semi arid (Fig. 1b) from south to north; summers have average temperatures of ~40–42 °C and occasionally reaches up to 47 °C. The winter (December–January) is short during which the minimum average temperature can reach ~15 °C, and may drop to 3–4 °C. The rainfall is restricted to 3 months (July–September), considered to be monsoon period. The annual rainfall distribution pattern is shown in Fig. 1d. The topography of the upland catchment is flat, as the Deccan lava flows have capped the older formations. The water received during the rainfall therefore easily flows

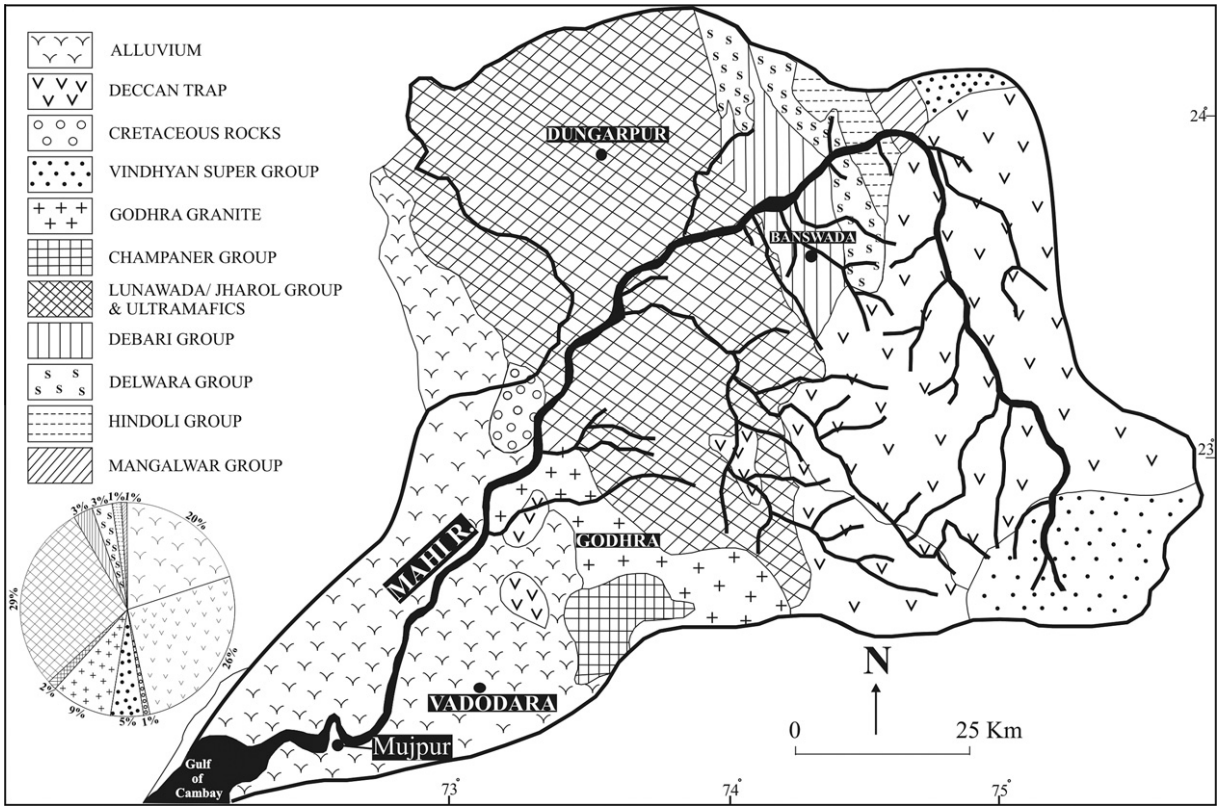


Fig. 2. Geological map of the Mahi River catchment showing exposed lithological units. The tributaries of the Mahi River mostly drain the Deccan province and the Precambrian crystallines of Rajasthan–Gujarat. The relative distribution of lithology is shown in the pi diagram.

through the river channel causing flash floods in the lower regions of the basin.

In summary, in a water-starved tectonically active terrain with resultant sea-level changes, the Mahi sediments may have been subjected to mechanical processes at the fluvio–marine interface.

## 3. METHODOLOGY

Approximately 8.5 m thick sedimentary sequence near Mujpur was systematically sampled. To minimize the effects of surface contamination and anthropogenic activity, the terrace's vertical face was trenched inward up to ~0.5 m. Depending on the observed physical heterogeneity of the weathered section (viz. variations in mineralogy, grain size, color, biologic activity, compactness), sampling was carried out at ~2 cm interval in the lower 3.72 m and at 5 cm interval in the upper 4.75 m of the section (Fig. 3). A total of 282 samples were collected, each in large quantities up to 1–1.5 kg. Samples were air dried in the laboratory prior to analytical work. In the bottom 1 m of the section, silty-sand and clay beds are more common. So the samples from this part of the section were collected at smaller intervals than those above. In the upper 4.75 m of the profile, however, the clay beds are sparse, and the sediment character gradually shifted to silty sand to fine sand. In the uppermost ~2 m of the section, the grain size is practically unimodal and of coarser sand sizes.

Textural analyses were performed on 52 selected samples. The samples were selected keeping in mind textural variations encountered in the Mujpur profile. About 10 g of samples were successively treated with sodium acetate, hydrogen peroxide and sodium citrate, sodium bicarbonate, and sodium dithionite to remove excess salts, carbonate, organic carbon and iron manganese coatings, respectively (Jackson, 1956; Knuze, 1965). The samples were then sieved through a 53 μ sieve (1000 μ = 1 mm) to remove sand (coarser) from the silt and clay (finer) fractions. Silt and clay fractions were then separated using a pipeting technique (Tanner and Jackson, 1947; Day, 1965).

In order to differentiate different clay mineral species (1:1 or 2:1 type), the clay fraction was separated into two parts. One part was saturated with potassium chloride and the other with calcium chloride solutions. The potassium-saturated clay-mounted slides were treated at different temperatures and calcium-saturated slides were glycolated prior to analyses using X-ray diffraction (Jackson, 1973). The cleaned sand fraction was observed with a hand lens and optical microscope before X-ray diffraction. The X-ray diffraction analysis was done at the Wadia Institute of Himalayan Geology (WIHG), Dehradun, Indian Institute of Technology (IIT), Roorkee and Jawaharlal Nehru University (JNU), New Delhi.

Samples were homogenized and crushed to about 200 mesh size in an agate mortar. The powdered samples were oven dried (~100 °C for 12 h), and pressed pellets were

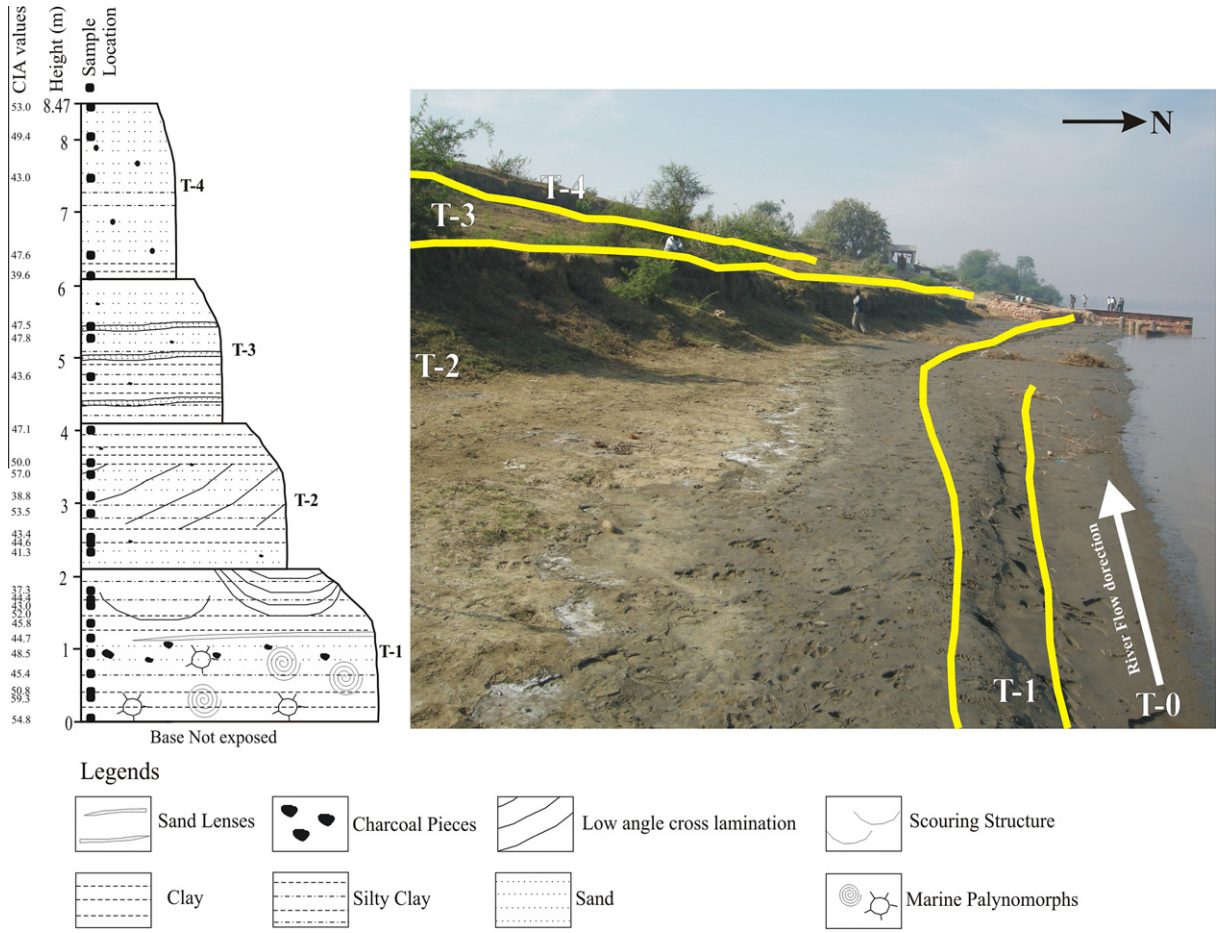


Fig. 3. Field photograph of the Mujpur section showing different terraces and the litholog with details of texture, sedimentary structure and distribution of organic matter. Sample locations (solid dots) in litholog (bottom to top) and corresponding CIA values of the samples shown (see Table 2 from left to right). The man (1.65 m) near the cliff is shown for scale.

prepared. The pellets were analyzed for major and minor elements using Wavelength dispersive XRF technique (Siemens SRS-3000) at WIHG, Dehradun. Details of the pellet preparation method are available elsewhere (e.g., Stork et al., 1987; Saini et al., 2000). The precision and accuracy of the sample preparation and instrumental performance were checked using several international reference standards of soil and sediments, e.g., SO-1, GSS-1, GSS-4, GXR-2, GXR-6, SCO-1, SGR-1, SDO-1, MAG-1, GSD-9, GSD-10, GSR-6 and BCS-267. The accuracy of measurement is better than 2–5% and precision <2% (see Purohit et al., 2010 for details).

Trace elements, including rare earth elements (REE), were analyzed by ICP-MS (PerkinElmer, Elan-DRCe), also at WIHG, Dehradun and IIT, Roorkee after digestion of the samples in Teflon crucibles using a mixture of $HF + HNO_3 + HClO_4$ acids by the 'B-solution' method (Shapiro and Brannock, 1962). The details of the procedure adopted for REE determination are given in Khanna et al. (2009). Several USGS standards (SGR-1, MAG-1, SCo-1) and a few in-house standards were used for machine calibration. Precision for ICP-MS analyses obtained is $\leqslant 5\%$.

## 4. RESULTS

### 4.1. Textures

The Mujpur sediment contains gradually increasing coarser fractions from the bottom to the top of the section. Thus, the lower 2.7 m is dominated by silt with periodic fine-sand horizons containing about ~10–20% clay. The middle part of the section (2.7–5.0 m) shows a gradual increase in sand with concomitant decrease in silt and clay fractions. The upper 3.5 m contains 60–70% sand and 25% silt (Fig. 4).

On the other hand, the more or less structure-less upper sandy portion of the section may be of aeolian origin. On a log ($Na_2O/K_2O$) vs. log ($SiO_2/Al_2O_3$) plot (Fig. 5) most samples plot as sublitharenite. In short, the Mujpur sediments show textural immaturity with some differences in depositional environments.

### 4.2. Mineralogy

Quartz, rock fragments, mafic minerals (pyroxene, biotite), and feldspar comprise the bulk sediment. Amongst

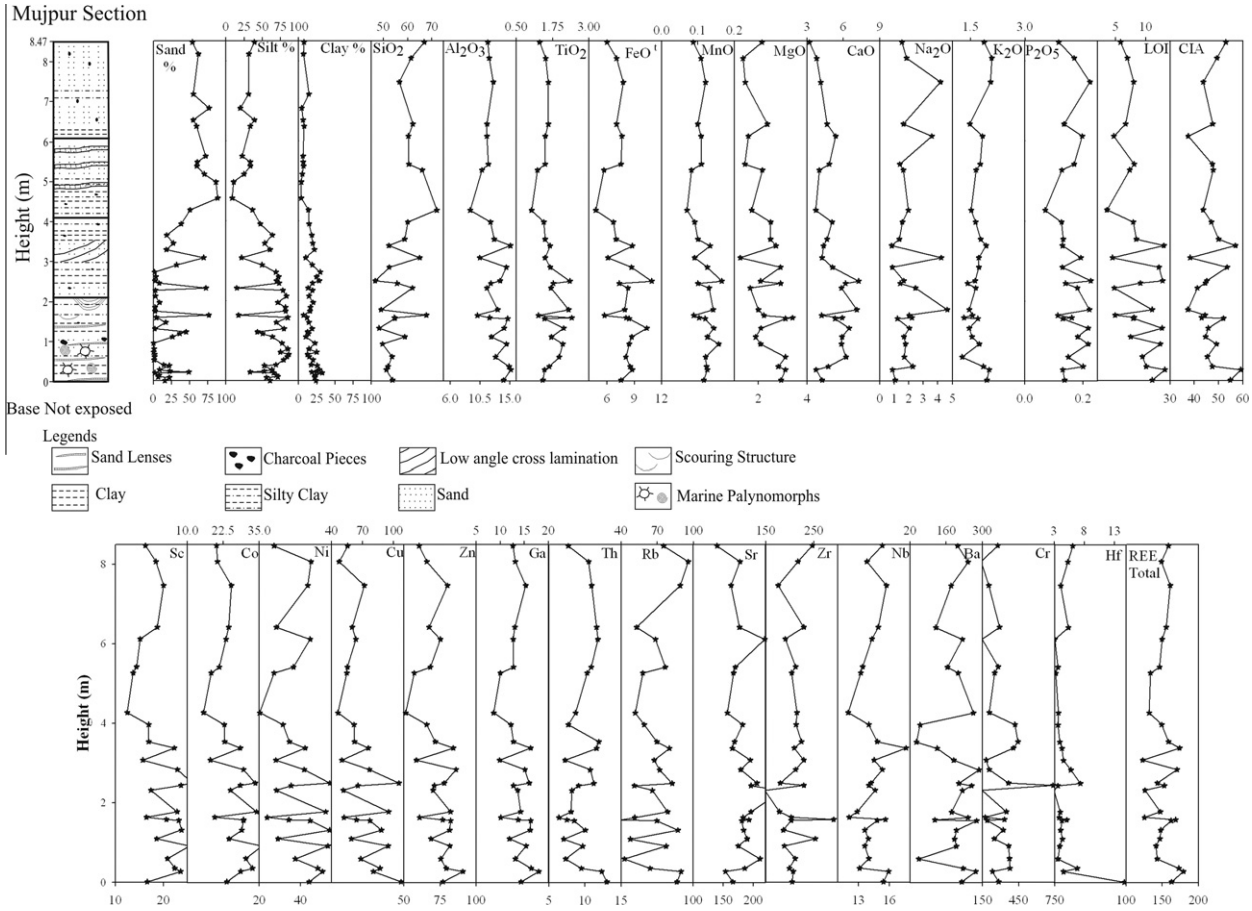


Fig. 4. Grain size (sand, silt ± clay) distributions in the Mujpur profile along with the litholog. Note that $SiO_2$ and felsic components are more in the coarser mode (coarse sand) wheras mafic components are enriched in the finer sediments.

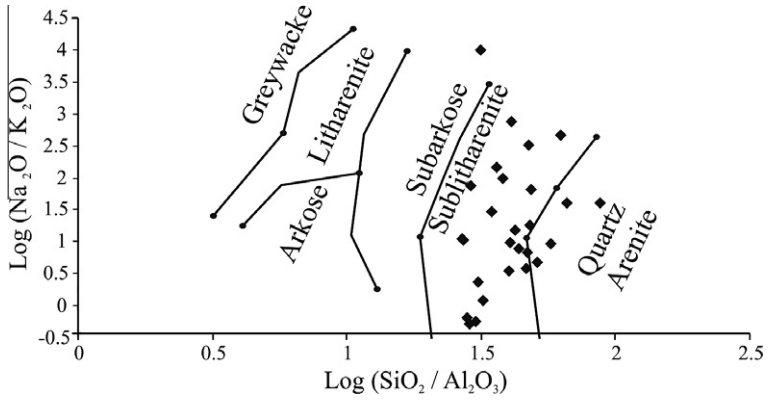


Fig. 5. Plot of $\log Na_2O/K_2O$ vs. $\log SiO_2/Al_2O_3$ (modified after Pettijohn et al., 1972) for the Mujpur samples. The samples plot in the sublitharenite field suggesting presence of lithic components in the bulk sediment.

clay minerals, smectite (50%) and illite (25%) with or without chlorite and kaolinite were identified using X-ray diffraction (XRD).

Thirteen thin sections of sand grains were also studied. About 400 grains were counted for modal analysis in each thin section. Quartz, basalt fragments (RF), biotite and pyroxene are the main detritus with lesser plagioclase and rare felsic rock fragments (banded gneiss) (Fig. 6).

The RFs are subangular to subrounded sand to coarse-sand. They contain plagioclase-phyric microporphyritic and/or vitrophyric textures with or without the presence of amygdules containing quartz, secondary silica and carbonates (Fig. 6).

The modal analyses of 13 samples are given in Table 1. Quartz and basalt fragments constitute the principal detrital mode (65–80%). Quartz occurs abundantly (>44%) or

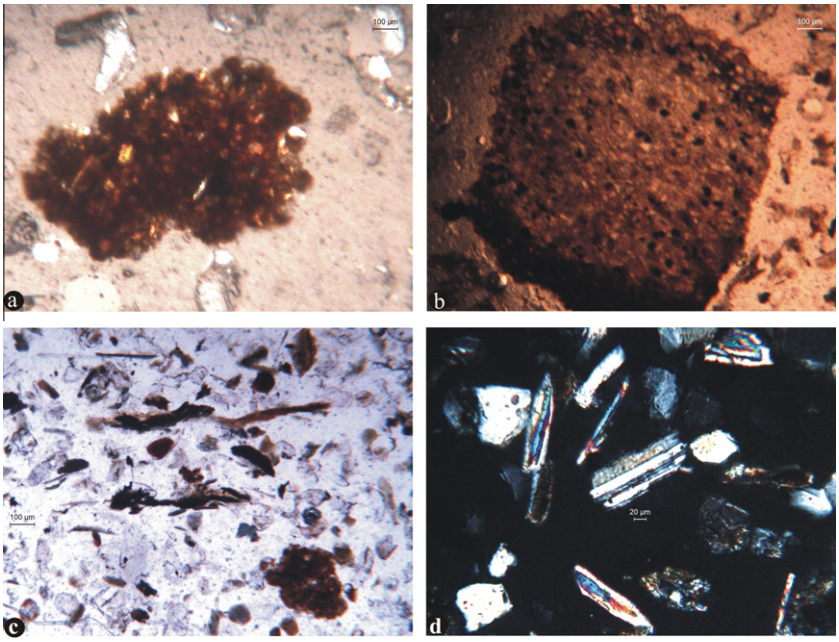


Fig. 6. (a) Pyroxene- and plagioclase-phyric basalt rock-fragment in Mujpur sediment. Irregular margin of the rock-fragment indicates short distance transportation. (b) Vesicular large basalt–fragment with irregular boundary in Mujpur sediment; vesicles filled with quartz, secondary silica and opaque minerals. (c) Brown to strong brown-colored biotite occur along length of the photograph (centre). Basalt-fragment is seen in right bottom; grains of quartz and feldspar occur in rest of the photograph. (d) Well-developed plagioclase lath with lamellar twining and mica in Mujpur sediment. (For interpretation of the references to colour in this figure legend, the reader is referred to the web version of this article.)

in sub-equal proportion to basalt fragments. In three samples, basalt fragment are more abundant than quartz. About 6–18% biotite occurs in the samples, and it shows a general increase with quartz, but is independent of the amount of basalt fragments. Pyroxene (<10%) is less abundant. Plagioclase is sparse (1–5%).

When plotted on quartz (Q)–feldspar (F)–lithic fragment (L) diagram, the samples plot mostly in the lithiarenite field (Fig. 7). The Mujpur sediments thus show mineralogical immaturity. The geologic setting in the upper reaches of the Mahi catchment (Fig. 2) testifies that the RF/pyroxene in the Mujpur samples have been derived from Deccan basalts.

Mineralogical and textural immaturity, coupled with predominance of smectite in the samples, supports water-starved condition, i.e. the arid/semi-arid climate prevalent in the region. Comparable X-ray diffraction patterns of both bulk and clay separates of the same samples suggest that there was no grain-size control for smectite formation and distribution. The difference in peak height in the XRD pattern may have been primarily governed by the dominant mode with increasing quartz (coarser fraction), which may have suppressed peak heights of other constituent minerals.

### 4.3. Geochemistry

#### *4.3.1. Major elements*

The major and trace element compositions for the Mujpur sediments are given in Table 2. The $SiO_2$ content of the samples range between 47 and 72 wt.%. The abundance of $SiO_2$, $FeO^t$ and $TiO_2$ are well correlated positively or negatively with $Al_2O_3$ (Fig. 8a–e). The MgO (2–3 wt.%), $Na_2O$ (1–2 wt.%), $K_2O$ (1.3–2 wt.%) and $P_2O_5$ (0.14 wt.%) content vary within a restricted range.

The samples are characterized by high $TiO_2$ ($\geqslant$1.4 wt.%) concentrations comparable to that of tholeiite (Table 2). Interestingly, Ca, known to be extremely mobile, does not show much depletion (CaO $\leqslant$ 7.25 wt.%), perhaps because release of silicate Ca is substantially lower (Lupker et al., 2012). Low concentrations ($Na_2O < 2$ wt.%) of extremely mobile Na may not necessarily indicate loss of Na from the system either, because of possible marine (Na-rich) influence in the Mujpur estuary. In an $Al_2O_3$ vs. $K_2O$ plot and a $FeO^t$ vs. $K_2O$ plot (Fig. 8f and g), samples have large variations in $FeO^t$ (5–11 wt.%) at nearly constant $K_2O$ (about 1.75 wt.%). The $K_2O$ concentration varies by at least a factor of two at similar $FeO^t$ in some samples, which may be attributed to variation in biotite.

Chemical alteration and mechanical breakdown of source rocks, followed by sorting of particles during transport, often leads to preferential enrichment of specific minerals in certain grain-size fractions. Therefore, sediment composition tends to be a function of grain size (Whitmore et al., 2004). When major element chemistry is studied in terms of grain size variations (Fig. 4), three important observations can be made: (1) sand-sized fraction increases up section, particularly in the upper 4.5 m of the section, and so does the $SiO_2$ content, (2) distribution patterns in finer fraction is complementary to that of the coarser sand fractions in the profile, and (3) distribution of $TiO_2$, $FeO^t$ and $Al_2O_3$ broadly follow the silt distribution patterns. Low $SiO_2$ (52–62 wt.%) and $Al_2O_3$ (13 wt.%), but slightly high CaO (>5 wt.%) suggest mafic sources for the Mujpur sediments (Table 2). Many samples have $TiO_2$

Table 1
Mineral modal analysis of sand fraction of the Mujpur samples.

| Sample No | MJ-15 | | MJ-31 | | MJ-80 | | MJ-83 | | MJ-117 | | MJ-123 | | MJ-126 | | MJ-218 | | MJ-221 | | MJ-235 | | MJ-262 | | MJ-274 | | MJ-282 | |
|---|---|---|---|---|---|---|---|---|---|---|---|---|---|---|---|---|---|---|---|---|---|---|---|---|---|---|
| Minerals | MC | % | MC | % | MC | % | MC | % | MC | % | MC | % | MC | % | MC | % | MC | % | MC | % | MC | % | MC | % | MC | % |
| Quartz | 192 | 48.1 | 191 | 37.5 | 157 | 55.1 | 185 | 59.3 | 248 | 44.0 | 176 | 36.7 | 130 | 28.1 | 152 | 41.3 | 151 | 41.6 | 296 | 50.5 | 199 | 39.3 | 267 | 50.5 | 207 | 48.3 |
| Feldspar (plagioclase) | 5 | 1.25 | 7 | 1.37 | 4 | 1.40 | 11 | 3.53 | 28 | 4.96 | 8 | 1.67 | 13 | 2.81 | 4 | 1.09 | 5 | 1.38 | 9 | 1.54 | 16 | 3.16 | 15 | 2.84 | 21 | 4.90 |
| Lithic | 117 | 29.3 | 228 | 44.7 | 33 | 11.6 | 66 | 21.2 | 96 | 17.0 | 240 | 50.0 | 250 | 54.1 | 80 | 21.7 | 57 | 15.7 | 207 | 35.3 | 180 | 35.6 | 130 | 24.6 | 130 | 30.3 |
| Biotite | 69 | 17.3 | 62 | 12.2 | 52 | 18.2 | 38 | 12.2 | 36 | 6.38 | 46 | 9.58 | 40 | 8.66 | 35 | 9.51 | 46 | 12.7 | 52 | 8.87 | 64 | 12.6 | 90 | 17.0 | 39 | 9.09 |
| Pyroxene | 16 | 4.01 | 22 | 4.31 | 39 | 13.7 | 12 | 3.85 | 156 | 27.7 | 10 | 2.08 | 29 | 6.28 | 97 | 26.4 | 104 | 28.7 | 22 | 3.75 | 47 | 9.29 | 27 | 5.10 | 32 | 7.46 |
| Total | 399 | | 510 | | 285 | | 312 | | 564 | | 480 | | 462 | | 368 | | 363 | | 586 | | 506 | | 529 | | 429 | |

MC = modal count, lithic: mafic volcanic rock fragment.

($\geqslant$1.4 wt.%) and $FeO^t$ (7.5–8.0 wt.%) comparable to that of mafic rocks (e.g., CFB-type rocks, see in Basaltic Volcanism Study Project, 1981), suggesting a possible mafic input. Elevated $SiO_2$ (>70 wt.%) in some samples attribute to increased contributions of quartzo–feldspathic sources. We do not find any systematic variation in CIA values (weathering index) in the sequence (Fig. 3). Also, an average CIA value (47.5) is close to that of 75% of the samples studied ($\sim$50), similar to unweathered rocks (50). In a short to medium-sized river like Mahi, we attribute finer grain size of $SiO_2$-poor and Fe–Ti–Ca rich detritus to fine-grained mafic source (Deccan basalts), rather than action of fluvial transport. In short, sand-sized minerals (e.g., quartz, feldspar) may have greater influence on sediment chemistry up section, but refractory elements i.e. Ti, Fe, Al are preferentially hosted in the silt fraction, that decrease up section. The Ti-, Fe- and Mn-rich sand grains occur to a limited extent in the transition stage roughly within 4–6 m.

#### 4.3.2. Trace elements

Relatively immobile trace elements like Cr, Ni and major-element oxides $Al_2O_3$ and $TiO_2$ undergo the least fractionation during sedimentary processes (Hessler and Lowe, 2006). Several of the Mujpur samples are enriched in Cr ($\geqslant$200 ppm) and Ni ($\geqslant$40 ppm) (Table 2) compared to those of UCC (Cr: 83 ppm, Ni: 44 ppm) (McLennan, 2001), and average shale (Cr: 104 ppm, Ni: 54 ppm; Condie, 1993). Good to reasonable positive correlations exist between $FeO^t$, MnO, $Al_2O_3$, $TiO_2$ and MnO with Ni, Co and Cr (Fig. 8h–m) in the suite suggesting significant mafic input. Interestingly, the lower-$SiO_2$ samples (49–55 wt.%) have higher concentrations of Cr (>250 ppm vs. <200 ppm), Ni (>40 ppm vs. <25 ppm), lower Th/Cr ($\leqslant$0.02), and lower Th/Sc (<0.6) and La/Sc, relative to the higher-$SiO_2$ samples (Fig. 8l–n). This clearly suggests that mafic phases primarily control transition element distributions in many samples, particularly in the lower part of the profile (Fig. 4). There is also a positive correlation between Cr contents and CIA values in the sediment samples (not shown).

The Sr concentrations in the samples vary positively with CaO (Fig. 8q), suggestive of plagioclase feldspar control. Less rainfall in the river catchment perhaps helped retention of plagioclase feldspar, and consequently Ca and Na, in the system. Immobile Ba and mobile Rb have positive correlation with $K_2O$ (Fig. 8r and s) and $Al_2O_3$ (not shown), which suggests alkali feldspar control. The nearly constant $K_2O$ (about 1.5 wt.%) and positive correlation of Rb with $FeO^t$ (Fig. 8g and t), and low Rb/Sr (<1), however, suggest biotite control, instead of alkali feldspar. The contribution of a boitite-rich, quartzo–feldspathic source (i.e. granitoid) is thus indicated. However, granitoid contributions may be restricted because of lower concentrations of K, Ba and Rb in the sediments.

#### 4.3.3. Rare earth elements (REE)

The chondrite-normalized plots of the rare earth elements (REE) (Fig. 9a), generally show higher concentrations of light REE (LREE) than heavy REE (HREE) with a negative Eu-anomaly similar to that of the upper

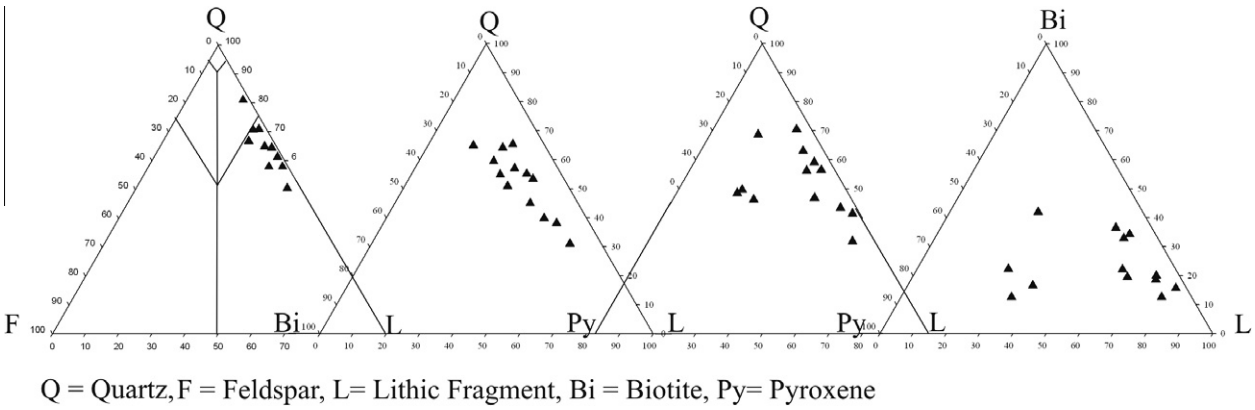


Fig. 7. On a Q (quartz)–F (feldspar)–L (lithic fragment) diagram, the Mujpur samples plot as sublithiarenite. Basalt fragments mostly represent lithics in the samples; pyroxene and biotite representing other mafic phases.

continental crust (UCC: McLennan, 2001), although with variable REE concentrations compared to the UCC. The ubiquitous negative Eu anomalies and high REE abundance with patterns similar to the UCC are, however, surprising for a mafic provenance.

The REE patterns of most shale are remarkably uniform: steep LREE slope, flat HREE, and slightly negative Eu anomaly. Interestingly, most of the Mujpur samples do not have REE patterns comparable to average shale or post-Archaean Australian Shale (PAAS). When normalized to PAAS, the samples have characteristically lower LREE, higher MREE (Sm–Dy) with a distinct positive Eu anomaly. The HREE (Yb–Lu), are comparable or slightly lower than that of PAAS, but with a slightly negative slope (Fig. 9b). When normalized to the UCC, samples reveal distinct REE patterns: consistently LREE depleted $(La/Yb)n < 1$) by about 2–4 times with or without a weak Sm–Eu–Gd plateau (Fig. 9c). A Few samples have slightly elevated LREE patterns, but with similarly low LREE/HREE ratios ($(La/Yb)n < 1$). The average of $Eu/Eu^*$ is 0.724 (0.70–0.75) which is slightly greater than the PASS and UCC ($PASS_{Eu/Eu^*} = 0.65, UCC_{Eu/Eu^*} = 0.70$), respectively. Nevertheless, the general uniformity in the REE pattern may be attributed to better mechanical mixing and increase in REE abundance in the finer fraction.

The higher-$TiO_2$ samples have characteristically low $(La/Yb)n$ (<1). Also the total REE concentrations increase with Cr, except for one sample with the highest Cr (>700 ppm) (Fig. 10). This kind of relationship is not common in sediments, and will be discussed in the following section.

## 5. DISCUSSION

The chemical composition of clastic sediments is a net result of a number of geological and possibly biological factors. These include nature of source rocks, intensity of chemical weathering, rate of sediment supply, and sorting (both textural and mineralogical) during transportation and deposition (Piper, 1974; McLennan, 1989; Cox and Lowe, 1995). Each of these factors must be evaluated before constraining the nature of the source rocks using mineralogy and chemistry of the clastic sediments. In this section, the sediment compositions are first considered that may have resulted due to or have been modified by weathering. Then the relative proportion of possible source rocks for the Mahi sediments is estimated.

### 5.1. Effects of marine action on sediment chemistry

As described above (Section 2), the Mujpur sediments were deposited in a transitional fluvio–marine environment. It is conceivable that erosion in the Mahi catchments may not have produced enough finer sediment (silt + clay). Fine-grained basaltic source rocks and/or mechanical action of marine winnowing at the fluvio–marine interface (estuaries/tidal flat) could be plausible reason(s) for the generation of the fine detritus.

With increased reworking, the immobile element Zr, may have become enriched in the sediments. The Th/Sc vs. Zr/Sc plot (McLennan, 2003) is useful in determining if such processes could affect the geochemical attributes of sediments. The Mujpur samples plot on the line joining basaltic (MORB), intermediate and UCC sources, but far away from the chemical trend of recycled sediments (Fig. 11a).

The possible dissolution of feldspars may have also occurred in our samples in marine waters. The plot in Fig. 11b shows that sea water with alkaline chemistry (pH = 7–8) is not conducive of feldspar dissolution. Low pH (pH 3) and high temperature are conducive for rapid dissolution of feldspars (Brantley, 2003 and references therein). Thus, marine action within the Mujpur estuary may have only partly imparted fineness to the detritus, but could not have affected its overall chemistry. This brings out important constraints that sediment characteristics in the Mujpur are typical of the Mahi catchments.

### 5.2. Weathering index and CIA pattern

To identify the effect of weathering and transport, the samples were plotted in the $Al_2O_3$–$(CaO + Na_2O)$–$K_2O$ (A–CN–K) and $Al_2O_3$–$(CaO + Na_2O + K_2O)$–$FeO^t$ + -MgO (A–CNK–FM) diagram (Fig. 12), along with the

Table 2
Major, trace and rare earth element compositions of the Mujpur sediments. Also given compositions of UCC, PAAS, average Tholeiite (Tho), Granitoid gneiss (BGC) and Siwalik siltstone/mudstone for comparision.

| | MJ-2 | MJ-15 | MJ-19 | MJ-31 | MJ-47 | MJ-56 | MJ-67 | MJ-79 | MJ-80 | MJ-83 | MJ-90 | MJ-117 | MJ-123 | MJ-126 | MJ-143 | MJ-155 | MJ-170 | MJ-178 | MJ-192 | MJ-207 | MJ-218 | MJ-221 | MJ-235 | MJ-241 | MJ-262 | MJ-274 | MJ-282 | UCC | PAAS | ThoΦ | BGC$ | Siwalik# |
|---|---|---|---|---|---|---|---|---|---|---|---|---|---|---|---|---|---|---|---|---|---|---|---|---|---|---|---|---|---|---|---|
| *Major oxide (wt %)* | | | | | | | | | | | | | | | | | | | | | | | | | | | | | | | |
| $SiO_2$ | 53.7 | 51.2 | 51.8 | 53.5 | 49.6 | 58.8 | 48.2 | 54.8 | 54.5 | 67.7 | 49.0 | 61.9 | 55.6 | 46.5 | 52.3 | 64.9 | 52.2 | 58.7 | 60.0 | 71.9 | 65.9 | 60.5 | 60.2 | 62.1 | 56.6 | 61.3 | 66.9 | 66.6 | 62.8 | 53.0 | 77.4 | 65.4 |
| $Al_2O_3$ | 14.1 | 15.2 | 14.9 | 12.9 | 14.5 | 12.2 | 14.1 | 14.7 | 11.9 | 10.1 | 13.2 | 11.5 | 12.1 | 13.6 | 14.5 | 10.5 | 15.1 | 12.7 | 12.1 | 9.02 | 10.8 | 11.8 | 11.5 | 11.6 | 12.5 | 11.9 | 11.7 | 15.4 | 18.9 | 13.1 | 11.7 | 15.8 |
| $TiO_2$ | 1.41 | 1.47 | 1.63 | 1.97 | 2.10 | 1.71 | 2.13 | 1.47 | 2.41 | 1.26 | 2.30 | 1.69 | 1.77 | 2.34 | 1.67 | 1.49 | 1.66 | 1.49 | 1.45 | 1.02 | 1.23 | 1.49 | 1.50 | 1.60 | 1.60 | 1.51 | 1.30 | 0.64 | 1.00 | 1.46 | 0.25 | 0.73 |
| $FeO^t$ | 7.53 | 8.76 | 8.54 | 8.05 | 8.40 | 8.71 | 10.4 | 8.41 | 8.09 | 5.71 | 7.94 | 8.29 | 7.34 | 10.9 | 8.67 | 6.09 | 8.76 | 6.96 | 6.69 | 4.75 | 5.66 | 7.51 | 7.63 | 7.04 | 7.76 | 7.02 | 5.98 | 5.04 | 7.08 | 13.6 | 0.85 | 5.88 |
| MnO | 0.12 | 0.13 | 0.12 | 0.12 | 0.16 | 0.13 | 0.14 | 0.12 | 0.10 | 0.09 | 0.14 | 0.13 | 0.10 | 0.17 | 0.13 | 0.09 | 0.13 | 0.10 | 0.09 | 0.07 | 0.08 | 0.11 | 0.11 | 0.10 | 0.12 | 0.11 | 0.09 | 0.10 | 0.11 | 0.21 | 0.02 | 0.06 |
| MgO | 2.93 | 3.10 | 2.81 | 3.10 | 2.07 | 1.88 | 2.10 | 3.11 | 3.40 | 2.22 | 1.99 | 1.65 | 2.91 | 2.08 | 2.90 | 1.24 | 2.72 | 2.49 | 2.50 | 1.72 | 2.15 | 1.44 | 1.58 | 2.36 | 1.45 | 1.36 | 2.14 | 2.48 | 2.20 | 6.29 | 0.52 | 2.59 |
| CaO | 4.25 | 3.74 | 4.77 | 6.23 | 5.84 | 5.89 | 6.48 | 5.33 | 5.90 | 4.21 | 7.10 | 5.84 | 6.18 | 7.25 | 5.10 | 4.25 | 4.36 | 4.66 | 5.08 | 3.73 | 4.02 | 4.84 | 5.37 | 4.64 | 4.13 | 3.79 | 3.19 | 3.59 | 1.30 | 7.81 | 0.93 | 1.60 |
| $Na_2O$ | 1.06 | 0.88 | 2.27 | 1.68 | 1.77 | 1.67 | 2.04 | 1.22 | 2.22 | 2.02 | 4.65 | 2.45 | 1.41 | 1.66 | 0.87 | 4.23 | 0.83 | 1.36 | 1.55 | 1.96 | 1.63 | 1.39 | 3.58 | 1.64 | 4.19 | 1.85 | 1.53 | 3.27 | 1.20 | 3.02 | 4.64 | 0.65 |
| $K_2O$ | 1.95 | 2.01 | 1.85 | 1.27 | 1.74 | 1.54 | 1.46 | 1.70 | 1.32 | 1.55 | 1.47 | 1.64 | 1.42 | 1.62 | 1.73 | 1.72 | 1.93 | 1.78 | 1.64 | 1.52 | 1.65 | 1.77 | 1.83 | 1.48 | 2.05 | 2.08 | 1.87 | 2.80 | 3.70 | 0.97 | 1.59 | 3.04 |
| $P_2O_5$ | 0.14 | 0.13 | 0.20 | 0.15 | 0.22 | 0.18 | 0.22 | 0.13 | 0.16 | 0.11 | 0.22 | 0.18 | 0.14 | 0.23 | 0.13 | 0.19 | 0.13 | 0.13 | 0.13 | 0.07 | 0.13 | 0.17 | 0.20 | 0.13 | 0.22 | 0.17 | 0.12 | 0.15 | 0.16 | 0.15 | 0.05 | 0.09 |
| LOI | 11.1 | 13.1 | 10.1 | 9.43 | 12.4 | 7.50 | 12.7 | 7.93 | 8.07 | 4.95 | 11.0 | 4.78 | 9.11 | 12.8 | 12.1 | 4.49 | 13.0 | 8.41 | 7.92 | 3.57 | 7.31 | 8.06 | 4.71 | 6.67 | 7.99 | 6.94 | 5.82 | NA | 6.00 | 1.48 | 0.45 | 5.31 |
| Total | 98.2 | 99.7 | 99.0 | 98.4 | 98.8 | 100.2 | 99.9 | 98.8 | 98.1 | 99.9 | 99.0 | 100.1 | 98.1 | 99.1 | 100 | 99.2 | 101 | 98.8 | 99.1 | 99.4 | 101 | 99.0 | 98.3 | 99.3 | 98.6 | 98.0 | 101 | 100 | 105 | 101 | 98.5 | 101 |
| *Trace element (ppm)* | | | | | | | | | | | | | | | | | | | | | | | | | | | | | | | |
| Ba | 220 | 274 | 225 | 54.0 | 199 | 192 | 200 | 278 | 116 | 244 | 181 | 223 | 258 | 209 | 287 | 189 | 125 | 45.0 | 59.0 | 265 | 206 | 165 | 223 | 120 | 179 | 244 | 204 | 628 | 650 | 251 | 265 | 474 |
| Co | 23.7 | 28.5 | 32.6 | 30.4 | 36.1 | 24.5 | 28.9 | 29.6 | 29.4 | 19.5 | 34.1 | 25.0 | 28.5 | 33.6 | 29.5 | 18.0 | 28.4 | 22.9 | 22.9 | 15.7 | 18.4 | 21.1 | 23.4 | 24.4 | 25.3 | 20.5 | 20.2 | 17.3 | 23.0 | NA | NA | 16.8 |
| Cr | 284 | 233 | 377 | 373 | 368 | 246 | 323 | 189 | 333 | 173 | 349 | 147 | 737 | 365 | 205 | 181 | 406 | 445 | 420 | 207 | 250 | 281 | 146 | 291 | 203 | 138 | 277 | 92.0 | 110 | 256 | 4.20 | 150 |
| Cu | 107 | 80.4 | 86.8 | 68.2 | 94.8 | 59.2 | 88.3 | 77.1 | 64.0 | 52.0 | 95.2 | 51.4 | 65.4 | 105 | 76.6 | 50.0 | 75.5 | 62.0 | 61.7 | 46.2 | 54.7 | 55.4 | 63.4 | 59.8 | 71.6 | 47.2 | 55.4 | 28.0 | 50.0 | NA | NA | 31.0 |
| Ga | 14.3 | 18.0 | 16.4 | 13.1 | 15.4 | 11.9 | 16.2 | 16.3 | 13.7 | 10.1 | 14.2 | 13.6 | 12.7 | 16.0 | 15.1 | 9.87 | 16.3 | 12.7 | 12.2 | 8.60 | 10.0 | 12.7 | 12.7 | 13.0 | 15.3 | 13.1 | 12.6 | 17.5 | 20.0 | 22.8 | 13.6 | 17.3 |
| Hf | 14.7 | 4.55 | 6.84 | 3.60 | 3.91 | 4.39 | 4.05 | 4.31 | 5.10 | 3.83 | 4.02 | 2.96 | 3.62 | 7.38 | 5.77 | 4.55 | 4.29 | 3.95 | 3.64 | 3.71 | 3.30 | 3.62 | 3.08 | 5.38 | 4.11 | 5.26 | 6.08 | 5.30 | 5.00 | NA | NA | NA |
| Nb | 15.4 | 15.9 | 13.1 | 14.0 | 13.6 | 13.9 | 13.6 | 14.8 | 15.6 | 12.1 | 12.9 | 14.6 | 14.0 | 14.2 | 15.3 | 14.5 | 17.6 | 14.8 | 14.0 | 12.0 | 13.2 | 13.4 | 14.3 | 14.9 | 15.7 | 13.8 | 15.3 | 12.0 | 19.0 | 7.00 | 13.4 | 14.5 |
| Ni | 44.1 | 50.5 | 48.2 | 37.4 | 53.2 | 29.0 | 54.1 | 44.5 | 34.2 | 23.8 | 52.2 | 28.3 | 35.4 | 54.2 | 41.7 | 28.0 | 42.2 | 34.5 | 31.4 | 20.2 | 27.1 | 36.6 | 44.6 | 28.2 | 43.5 | 45.1 | 27.1 | 47.0 | 55.0 | 98.8 | 2.03 | 57.7 |
| Pb | 16.1 | 19.6 | 14.7 | 9.00 | 17.6 | 12.9 | 17.5 | 12.5 | 9.40 | 16.3 | 15.3 | 12.7 | 12.1 | 16.1 | 14.4 | 16.9 | 13.7 | 15.2 | 18.0 | 14.8 | 16.1 | 13.0 | 17.2 | 14.6 | 14.4 | 14.3 | 17.4 | 17.0 | 20.0 | NA | NA | 24.3 |
| Rb | 86.2 | 89.7 | 64.0 | 42.7 | 77.2 | 47.6 | 87.1 | 69.6 | 39.9 | 51.1 | 78.6 | 65.8 | 50.8 | 82.4 | 71.9 | 67.5 | 79.9 | 69.6 | 59.1 | 51.7 | 57.9 | 76.5 | 68.4 | 52.8 | 88.9 | 95.6 | 75.2 | 84.0 | 160 | 30.4 | 27.8 | 140 |
| Sc | 16.6 | 23.6 | 22.3 | 20.8 | 25.5 | 18.6 | 23.8 | 23.2 | 20.6 | 16.5 | 22.9 | 17.4 | 23.7 | 26.1 | 22.9 | 15.7 | 22.3 | 16.9 | 17.0 | 12.5 | 13.7 | 14.4 | 15.2 | 18.7 | 20.0 | 18.4 | 16.3 | 14.0 | 16.0 | NA | NA | 15.0 |
| Sr | 166 | 154 | 186 | 211 | 175 | 190 | 184 | 181 | 193 | 183 | 196 | 247 | 196 | 206 | 179 | 195 | 165 | 169 | 182 | 157 | 167 | 170 | 219 | 177 | 163 | 178 | 140 | 320 | 200 | 169 | 81.0 | 87.1 |
| Th | 13.0 | 12.3 | 9.50 | 7.30 | 9.66 | 7.05 | 10.1 | 8.50 | 7.50 | 6.40 | 8.08 | 8.18 | 9.10 | 11.2 | 10.7 | 7.23 | 11.6 | 11.9 | 7.70 | 8.70 | 10.3 | 10.9 | 11.8 | 11.6 | 10.9 | 10.5 | 7.7 | 10.5 | 14.6 | 5.10 | 14.0 | 14.2 |
| U | 1.71 | 2.07 | 1.92 | 1.80 | 1.54 | 1.80 | 1.61 | 1.89 | 2.02 | 1.53 | 1.55 | 1.70 | 1.90 | 1.49 | 1.81 | 1.48 | 1.72 | 1.83 | 1.34 | 1.63 | 1.56 | 1.55 | 1.73 | 1.79 | 1.86 | 1.52 | 1.86 | 2.70 | 3.10 | NA | NA | 3.02 |
| V | 161 | 183 | 175 | 197 | 202 | 197 | 208 | 192 | 249 | 165 | 205 | 152 | 173 | 195 | 194 | 178 | 190 | 168 | 164 | 138 | 160 | 163 | 152 | 196 | 178 | 148 | 159 | 97.0 | 150 | 266 | 12.4 | 132 |
| Y | 36.8 | 35.7 | 28.9 | 34.2 | 30.7 | 33.8 | 28.9 | 37.0 | 38.9 | 29.0 | 31.5 | 24.2 | 34.8 | 27.1 | 37.2 | 18.9 | 36.3 | 32.7 | 31.9 | 28.2 | 26.7 | 22.2 | 23.2 | 37.9 | 24.7 | 23.5 | 41.7 | 21.0 | 27.0 | 27.3 | 34.4 | 35.0 |
| Zn | 77.0 | 90.8 | 79.3 | 75.5 | 81.8 | 68.7 | 81.7 | 82.3 | 76.8 | 60.8 | 82.2 | 70.1 | 71.0 | 77.9 | 86.0 | 58.6 | 84.1 | 71.6 | 65.7 | 51.2 | 57.2 | 68.2 | 75.2 | 67.4 | 80.1 | 65.8 | 60.6 | 67.0 | 85.0 | 152 | 13 | 86.2 |
| Zr | 205 | 207 | 199 | 211 | 189 | 253 | 186 | 203 | 291 | 203 | 178 | 148 | 229 | 180 | 212 | 229 | 209 | 224 | 213 | 215 | 204 | 212 | 191 | 229 | 176 | 217 | 247 | 193 | 210 | 146 | 206 | 232 |
| *REE (ppm)* | | | | | | | | | | | | | | | | | | | | | | | | | | | | | | | |
| La | 34.8 | 38.0 | 36.8 | 29.0 | 30.5 | 31.4 | 30.6 | 34.2 | 35.9 | 26.9 | 30.6 | 25.3 | 32.7 | 28.4 | 35.9 | 25.9 | 36.2 | 34.6 | 31.4 | 27.7 | 29.6 | 31.2 | 33.1 | 33.7 | 34.7 | 32.5 | 34.3 | 31.0 | 38.0 | 19.4 | 30.2 | 47.0 |
| Ce | 73.8 | 80.2 | 73.5 | 60.0 | 62.7 | 63.2 | 62.8 | 70.1 | 71.7 | 54.6 | 62.9 | 53.1 | 69.2 | 61.2 | 73.5 | 53.6 | 75.0 | 69.4 | 64.9 | 57.6 | 58.7 | 64.3 | 65.2 | 67.3 | 70.2 | 65.2 | 70.1 | 63.0 | 80.0 | 38.8 | 63.0 | 98.6 |
| Nd | 29.6 | 33.6 | 34.4 | 29.2 | 25.7 | 28.7 | 28.7 | 31.2 | 33.2 | 24.0 | 29.1 | 26.1 | 27.9 | 29.1 | 34.1 | 24.0 | 34.8 | 30.6 | 29.6 | 26.7 | 25.3 | 28.0 | 28.3 | 29.9 | 31.6 | 28.8 | 30.2 | 27.0 | 32.0 | 19.5 | 25.7 | 39.3 |
| Sm | 6.53 | 7.13 | 7.05 | 6.07 | 5.61 | 6.01 | 6.42 | 6.59 | 6.92 | 5.09 | 6.71 | 5.11 | 5.89 | 6.29 | 7.00 | 4.98 | 7.09 | 6.13 | 6.03 | 5.16 | 5.30 | 6.06 | 5.99 | 6.32 | 6.21 | 6.25 | 6.12 | 4.70 | 5.60 | 4.82 | 5.27 | 7.92 |
| Eu | 1.44 | 1.54 | 1.55 | 1.38 | 1.30 | 1.33 | 1.43 | 1.52 | 1.53 | 1.12 | 1.44 | 1.18 | 1.32 | 1.37 | 1.55 | 1.11 | 1.63 | 1.41 | 1.36 | 1.12 | 1.15 | 1.29 | 1.38 | 1.41 | 1.44 | 1.32 | 1.36 | 1.00 | 1.10 | 1.49 | 1.00 | 1.53 |
| Gd | 5.55 | 6.30 | 6.52 | 5.41 | 5.15 | 5.44 | 5.62 | 5.98 | 6.46 | 4.40 | 5.62 | 4.98 | 5.21 | 5.38 | 6.10 | 4.26 | 6.23 | 5.54 | 5.25 | 4.36 | 4.48 | 5.26 | 5.41 | 5.60 | 5.62 | 5.01 | 5.42 | 4.00 | 4.70 | 5.10 | 4.74 | 6.11 |
| Dy | 5.30 | 6.01 | 6.41 | 5.80 | 5.01 | 4.92 | 6.03 | 5.98 | 6.30 | 4.28 | 5.03 | 4.80 | 4.98 | 5.63 | 5.77 | 4.18 | 6.10 | 5.28 | 5.08 | 4.30 | 4.33 | 4.96 | 4.88 | 5.27 | 5.33 | 4.84 | 5.01 | 3.90 | 4.40 | 4.76 | 3.92 | 5.68 |
| Er | 3.02 | 3.35 | 3.49 | 3.15 | 2.82 | 3.02 | 3.26 | 3.52 | 3.43 | 2.59 | 3.09 | 2.88 | 2.86 | 3.10 | 3.36 | 2.60 | 3.47 | 2.94 | 3.02 | 2.39 | 2.48 | 2.77 | 2.77 | 2.99 | 2.99 | 2.60 | 3.01 | 2.30 | 2.90 | 2.69 | 2.17 | 3.36 |
| Yb | 2.53 | 2.95 | 2.87 | 2.68 | 2.39 | 2.52 | 2.70 | 2.95 | 2.81 | 2.25 | 2.59 | 2.41 | 2.48 | 2.60 | 2.81 | 2.16 | 2.93 | 2.50 | 2.51 | 2.23 | 2.13 | 2.30 | 2.41 | 2.55 | 2.57 | 2.17 | 2.62 | 1.96 | 2.80 | 2.29 | 2.07 | 2.95 |
| Lu | 0.42 | 0.46 | 0.45 | 0.42 | 0.39 | 0.41 | 0.41 | 0.45 | 0.45 | 0.36 | 0.39 | 0.39 | 0.38 | 0.38 | 0.46 | 0.34 | 0.48 | 0.40 | 0.40 | 0.34 | 0.34 | 0.37 | 0.39 | 0.43 | 0.42 | 0.36 | 0.46 | 0.31 | 0.43 | 0.32 | 0.29 | 0.44 |
| Th/Cr | 0.05 | 0.05 | 0.03 | 0.02 | 0.03 | 0.03 | 0.03 | 0.04 | 0.02 | 0.04 | 0.02 | 0.06 | 0.01 | 0.03 | 0.05 | 0.04 | 0.03 | 0.03 | 0.02 | 0.04 | 0.04 | 0.04 | 0.08 | 0.04 | 0.05 | 0.08 | 0.03 | 0.11 | 0.13 | 0.02 | 3.33 | 0.10 |
| La/Sc | 2.09 | 1.61 | 1.65 | 1.39 | 1.20 | 1.69 | 1.29 | 1.48 | 1.74 | 1.63 | 1.34 | 1.45 | 1.38 | 1.09 | 1.57 | 1.65 | 1.62 | 2.04 | 1.85 | 2.21 | 2.15 | 2.17 | 2.18 | 1.80 | 1.73 | 1.77 | 2.11 | 2.21 | 2.38 | NA | NA | 3.14 |
| Th/Sc | 0.78 | 0.52 | 0.43 | 0.35 | 0.38 | 0.38 | 0.42 | 0.37 | 0.36 | 0.39 | 0.35 | 0.47 | 0.38 | 0.43 | 0.47 | 0.46 | 0.52 | 0.70 | 0.45 | 0.70 | 0.75 | 0.75 | 0.78 | 0.62 | 0.54 | 0.57 | 0.47 | 0.75 | 0.91 | NA | NA | 0.95 |
| Zr/Y | 5.58 | 5.79 | 6.89 | 6.16 | 6.16 | 7.49 | 6.45 | 5.49 | 7.48 | 7.00 | 5.65 | 6.09 | 6.59 | 6.64 | 5.69 | 12.14 | 5.75 | 6.85 | 6.67 | 7.64 | 7.63 | 9.55 | 8.23 | 6.05 | 7.13 | 9.23 | 5.93 | 9.19 | 7.78 | 5.34 | 5.98 | 6.63 |
| La/Sm | 5.32 | 5.33 | 5.22 | 4.77 | 5.44 | 5.22 | 4.76 | 5.19 | 5.19 | 5.28 | 4.56 | 4.94 | 5.55 | 4.52 | 5.13 | 5.20 | 5.10 | 5.64 | 5.21 | 5.37 | 5.58 | 5.16 | 5.52 | 5.33 | 5.58 | 5.20 | 5.60 | 6.60 | 6.79 | 4.03 | 5.73 | 5.94 |
| La/Yb | 13.7 | 12.9 | 12.8 | 10.8 | 12.8 | 12.4 | 11.3 | 11.6 | 12.8 | 11.9 | 11.8 | 10.5 | 13.2 | 10.9 | 12.8 | 12.0 | 12.3 | 13.8 | 12.5 | 12.4 | 13.9 | 13.6 | 13.7 | 13.2 | 13.5 | 15.0 | 13.1 | 15.8 | 13.6 | 8.48 | 14.6 | 15.9 |
| $Eu/_{Eu}^*$ | 0.73 | 0.70 | 0.70 | 0.74 | 0.74 | 0.71 | 0.73 | 0.74 | 0.70 | 0.72 | 0.71 | 0.71 | 0.73 | 0.72 | 0.73 | 0.73 | 0.75 | 0.74 | 0.74 | 0.72 | 0.72 | 0.70 | 0.74 | 0.72 | 0.74 | 0.72 | 0.72 | 0.70 | 0.65 | 0.92 | 0.61 | 0.67 |
| CIA | 54.8 | 59.3 | 50.8 | 45.4 | 48.5 | 44.7 | 45.8 | 52.0 | 43.0 | 44.4 | 37.3 | 41.3 | 44.6 | 43.4 | 53.5 | 38.8 | 57.0 | 50.0 | 47.1 | 43.6 | 47.8 | 47.5 | 39.6 | 47.6 | 43.0 | 49.4 | 53.0 | 50.8 | 69.4 | 39.3 | 51.4 | 68.6 |

ThoΦ: Tholeiitic Basalt (avg. 10 samples) and BGC$: Banded Gneissic Complex (avg. 5 samples) (Ahmad and Tarney, 1994); Siwalik# (avg. 51 samples for major & trace elements; avg. 22 samples for REE) (Sinha et al., 2007); Upper Continental Crust (UCC) (Rudnick and Gao, 2003); Post-Archaean Australian Shale (PAAS), (Taylor and McLennan, 1985).

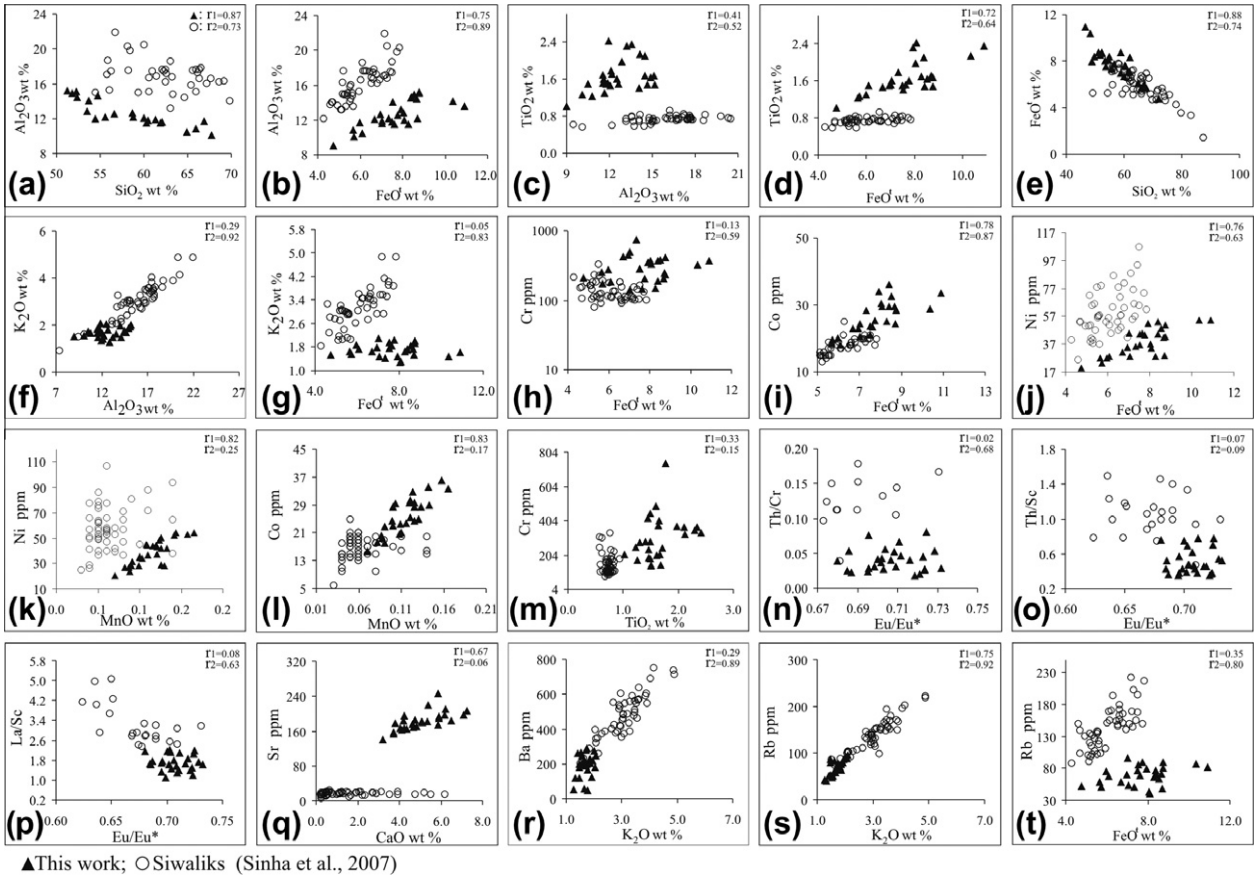


Fig. 8. Binary plots showing relations among different major oxides and trace elements for the Mujpur samples. Compositions of the Siwalik mudstone/siltstone (Sinha et al., 2007) are plotted for comparison. For details, see text.

chemical index of alteration (CIA: Nesbitt and Young, 1989). The CIA indicates the degree of chemical weathering and is defined as $[Al_2O_3/(Al_2O_3 + CaO + Na_2O + K_2O) \times 100]$ in molecular proportions, where CaO is from the silicates only. The CIA of the sediments ranges from 37 to 59 with the majority of the samples plotting around 45–54 in the A–CN–K plot (Fig. 12a). On an A–CNK–FM plot (Fig. 12b), the samples plot along the feldspar-biotite join, near the field of basalt.

The CIA of sediments is, in general, about 50 for first-cycle sediments that were dominantly derived from physically weathered igneous rocks and it tends to increase as chemical weathering intensifies (Nesbitt and Young, 1984). The CIA of the Mujpur samples $\leqslant 50$ (UCC $\sim$ 50) clearly suggests the sediment has experienced minimal chemical weathering. The presence of less-weathered rocks in semi-arid conditions is also supported by field observation.

In summary, the low CIA values in our samples can be attributed to the influx of minimally weathered detritus in a tectonically active and water-starved semi-arid condition. The tectono–climatic condition thus promoted enhanced erosion (mechanical process), but inhibited chemical weathering in the Mahi catchment. The presence of abundant physical heterogeneity (e.g., gneissic fabric, fractures, joint planes, and shear planes) in the upland rocks may have been conducive for water runoff during flash flooding to percolate through source rocks causing limited chemical weathering (CIA up to 59).

### 5.3. Source rock characteristics

#### 5.3.1. Evidence from ferromagnesian transition metals

Ferromagnesian elements (e.g., Fe, Cr, Co and Ni) are enriched in mafic and ultramafic igneous rocks and elevated abundances of these elements in the sediments and sedimentary rocks may indicate the addition of components derived from mafic rocks (Bock et al., 1998 and references therein). Elevated Cr and Ni abundances with low Cr/Ni ratios (1.3–1.5) were further suggested to be indicative of ultramafic rocks in the source area of shales (Garver et al., 1996). Although high Cr and Ni contents suggest a mafic/ultramafic provenance, ultramafic rocks can attain Cr/Ni ratios $\geqslant 10$ (Jaques et al., 1983) and accordingly, the low Cr/Ni ratios need not be indicative of an ultramafic provenance (Bock et al., 1998). Thus, the elevated Cr and Ni abundances (Cr > 250 ppm, Ni > 45 ppm) and Cr/Ni ratios (>5) in many Mujpur samples and their positive correlation with $FeO^t$ and $TiO_2$ further confirm that mafic lithologies must have contributed to sediment formation. Lower Y/

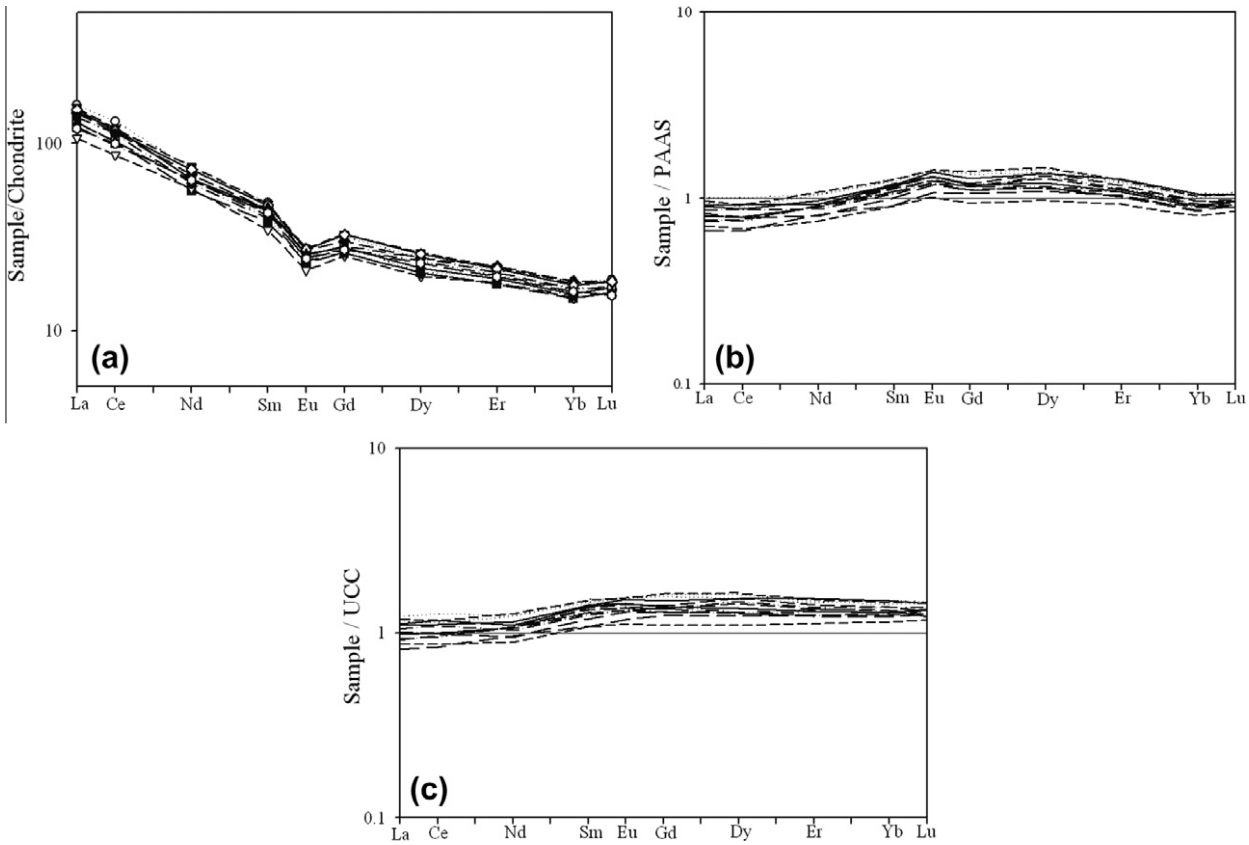


Fig. 9. REE patterns for the Mujpur samples. (a) Chondrite-normalized REE plots showing UCC pattern, (b) PAAS-normalized REE patterns showing less fractionated character with depleted LREE, but with positive Eu-anomaly; HREE almost parallel to slightly depleted, and (c) UCC-normalized REE patterns with characteristic depleted LREE with a weak Eu-plateau; HREE is almost similar to UCC. *Sources:* chondrite (McDonough and Sun, 1995), UCC (Rudnick and Gao, 2003) and PAAS (Taylor and McLennan, 1985).

Ni ratios (<0.8) also suggests contributions from mafic source rocks, but probably not from ultramafic sources.

*5.3.2. Evidence from rare earth elements (REE)*

The REE pattern, however, is more interesting. The low LREE/HREE (<1) pattern (Fig. 9C) indicate that less differentiated materials than the UCC were supplied into the sediments. These REE patterns occur particularly in those samples which have higher Cr, and Ni concentrations and higher CIA values (up to 59). This clearly suggests: (a) the samples with low LREE/HREE (<1) pattern must have been derived from the mafic sources in the upper Mahi reaches. The more weatherable character of the basaltic provenance (Deccan basalts) may also support a higher CIA values for these samples. This type of REE pattern cannot be produced by chemical weathering, as the weathered product would normally increase the LREE content. This further suggests that chemical weathering of the mafic rocks, however incipient, did not control the REE pattern. So the REE pattern, in addition to major and some trace elements, of the samples, are characteristics of their source. Similar REE patterns (LREE/HREE < 1) were earlier obtained in sediments having been derived from largely mafic sources in the Cauvery catchment in southern India (Senssarma et al., 2008).

The HREE pattern, however, deserves some attention. The HREE pattern is almost parallel and unfractionated with respect to the UCC (except for the negative Eu-plateau), which clearly suggest a UCC-type source composition for these samples. The lower HREE concentrations occur in samples with abundant coarser faction (sand). The lower HREE abundance compared to the UCC by about 2–4 times may be attributed to the quartz dilution effect. The presence of garnet could have elevated the HREE concentrations in sediments, but cannot simultaneously explain the higher Cr, Co, Ni and Ti in those samples.

The weak Eu-plateau in the samples may suggest the presence of plagioclase + pyroxene. Plagioclase typically shows positive Eu-anomaly. On the other hand, pyroxenes have negative Eu-anomalies (see in Hanson, 1978). Relatively more role of plagioclase perhaps resulted in an overall weak Eu-plateau in the bulk samples (Fig 9b and c). This corroborates our observation that the sediments are relatively fresh and have experienced only mechanical weathering of predominantly of mafic and some granitoid sources.

*5.3.3. Relative contributions of mafic and felsic sources*

In order to better understand the relative contributions of different source materials, two likely potential sources, the Deccan tholeiitic basalts and Archean granitoids in

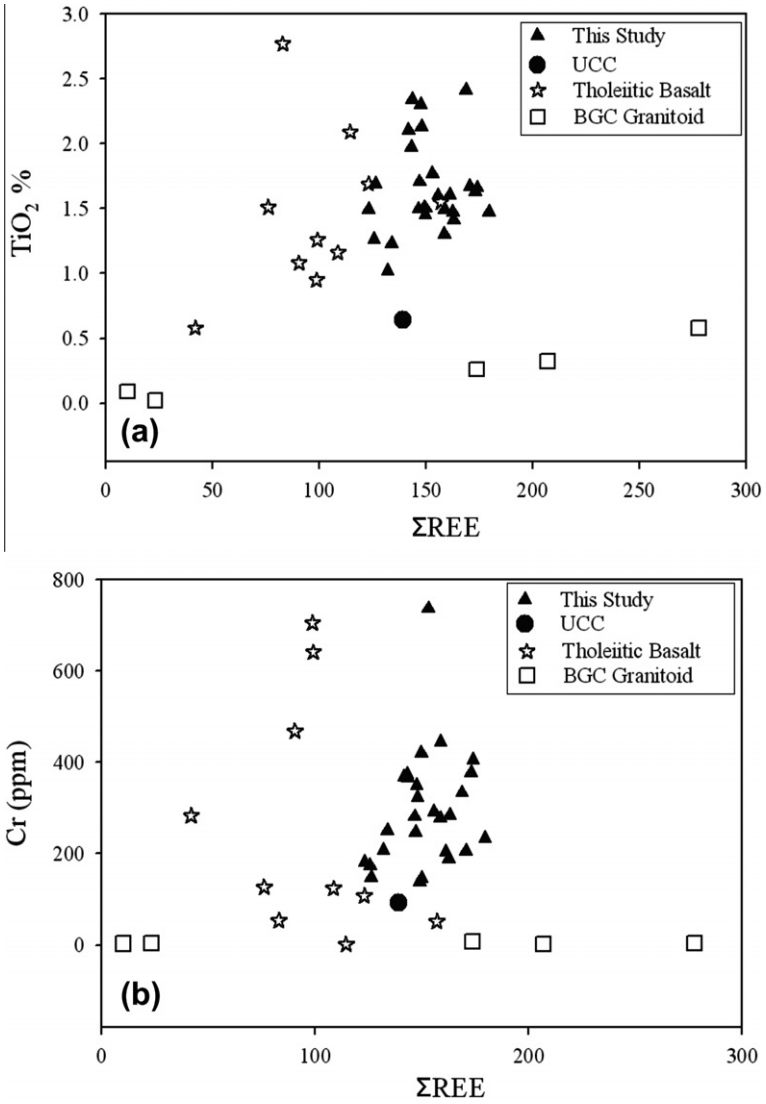


Fig. 10. (a) Total REE (ΣREE) vs. $TiO_2$ (wt.%) plot showing comparable or slightly lesser total REE concentrations in samples and Tholeiitic basalt (Ahmad and Tarney, 1994) at given $TiO_2$ (1–2.4 wt.%). Note granitoid (Ahmad and Tarney, 1994) have larger spread in REE concentrations at a given $TiO_2$ (0.05 wt.%). (b) Total REE (ΣREE) vs. Cr (ppm) plot showing similar Cr (200–400 ppm) samples and Tholeiitic basalt. Granitoid have large spread in total REE values at a much lesser Cr concentration (∼<10 ppm).

the Aravalli Craton are used as potential end member source components. A simple mixing between the tholeiitic basalts and the granitoids (BGC) was carried out. The measured concentration of a given element E in the bulk sediment sample, $C_{E,}$ is considered to be the sum of the concentration in tholeiitic source ($C_{Tho}$) and in the granitoid $C_E$ (felsic granitoid source $C_{BGC}$).

$$X_{Tho}C_E(\text{Tholeiite}) + X_{BGC}C_E(\text{BGC}) = C_E(\text{bulk sediment sample}), \quad (1)$$

where $X_{Tho}$ and $X_{BGC}$ are the fractions of basaltic tholeiite and BGC sources, respectively, and $X_{Tho} + X_{BGC} = 1$.

In Table 3, we present the mass balance calculations. From this table, it is clear that sub-equal proportions of tholeiite and granitoid BGC leads to compositions comparable to the average Mujpur samples, particularly for $Al_2O_3$, $FeO^t$, MgO, MnO, CaO and $P_2O_5$. The $SiO_2$, $TiO_2$ and $K_2O$ concentrations give better matches with large contributions from tholeiite (about 70–75%).

The trace elements comparisons are, however, more uncertain. For example, while Cr, and Sr concentrations call for mostly basaltic sources, the Ni content in the average Mujpur sediments can reasonably be accounted for with sub-equal input of both tholeiite and felsic granitoid sources. The Th and Zr concentrations are, expectedly, principally derived from granitoid sources, but do not match the Rb and Ba concentrations. Variable REE contributions of both the sources may reasonably explain the average REE budget in the sediments. Some of the spread in trace element contents, however, may also be related to large variations in concentrations of these elements in both the sources. Given these uncertainties, a reasonable fit for major and selected trace elements (Cr, Ni, Sr, La, Yb) is ob-

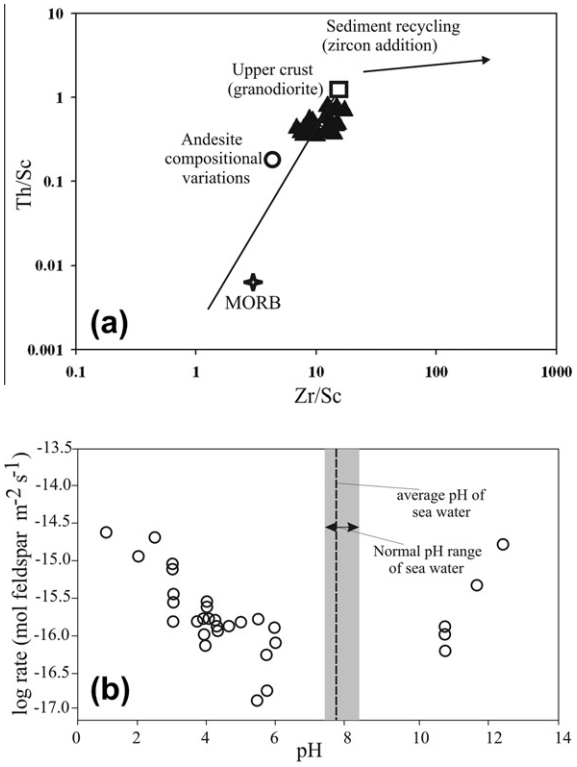


Fig. 11. (a) The Th/Sc vs Zr/Sc plot to show the effect of degree of reworking on the sediment geochemistry (after McLennan, 2003). The Mujpur sediments plot on the basalt-UCC join, more close to UCC, indicating retention of original characteristics of the sediments. (b) Log rate mol feldspar (dissolution rate) vs. pH plot indicating feldspar remain chemically unaffected by marine action. The figure and data taken from Brantley et al. (2003) and references therein.

tained by mixing ~70–75% of mafic end-member with ~25–30% of felsic end-member to produce the Mujpur bulk sediments.

On a Th–La–Ni plot (Fig. 13a), BGC (granitoids) and Deccan tholeiite are shown along with our samples. Our samples plot halfway along the La–Ni side, but clearly away from Th apex. On a Th–La–Cr diagram (Fig. 13b), our samples plot within the field of tholeiite. This clearly reiterates the predominant contributions of mafic sources in Mujpur sediments. Fineness of detritus in Mahi samples is primarily of the source characteristics, as discussed in Section 5.1. So, the Mujpur sediments may have still relatively higher contributions from the Deccan basalts. The tributaries meeting the Mahi River are essentially flowing through the Deccan province (Fig. 2) and are thus likely to sample the Deccan basalts.

### 5.4. Application to the Siwalik sedimentary rocks

In this section, the results of the Mahi alluvial samples are applied to the Neogene Siwalik siltstone and mudstone (Fig. 8) to test if the source characteristics and weathering of alluvium in sedimentary rocks can be ascertained. The Siwalik rock-system was selected for two reasons. First of all, diagenesis of sediments may significantly mobilize or fractionate REE and other trace elements leading to difficulties in linking chemical signatures to that of potential source(s) (e.g., Bloch and Hutcheon, 1992; Awwiller, 1993; Abanda and Hennigan, 2006). This problem is circumvented in case of young Siwalik sediments. Secondly, tracing the source characteristics of these rocks by geochemical methods is lacking, except for Sinha et al. (2007). A mixed provenance of granite gneiss/pelites, mafic rocks and sedimentary rocks with dominant felsic contributions is suggested by Sinha et al. (2007).

In Fig. 14, we evaluate chemical fractionation of trace elements in the Mahi samples and Siwalik rocks relative to the UCC (Rudnick and Gao, 2003). Higher concentrations of incompatible elements and REE (e.g., Rb, U, Th, Pb, La, Ce), and lower concentrations of compatible elements (e.g., Co, Cr, Ni, Cu) in the Siwaliks compared to the Mahi samples is apparent. Our samples are rich in Co, Cr, Ti, Cu contents. A reasonable match is made for $SiO_2$, $TiO_2$, $FeO^t$, MgO, Ni and Cr in the Siwalik rocks (aver) with sub-equal proportions of mafic and granitoid sources (Table 3). Incompatible elements (e.g., Ba, Rb, Sr, Zr, Yb, Eu), however were mostly supplied by granitoid sources.

The spread of U (1.34–2.07 ppm) in the Siwalik rocks could partly be attributed to the heterogeneity of granitoid sources of Sinha et al. (2007), and partly to more mobile character of U compared to Th. On the other hand, a strong Ba-negative anomaly and low Rb/U (<1) in our samples is characteristic and may indicate little or no alkali feldspar control in the Mahi source, unlike that of the Siwaliks. This is consistent with the presence of biotite–plagioclase–rich granitoid (BGC) in the Mahi source, as discussed earlier. However, a negative Sr-anomaly both in our samples and the Siwaliks suggest plagioclase-depleted sources. This may be consistent with granitoid sources for the Siwaliks, but not with the Mahi sediments.

The basaltic (high MgO) provenance is consistent with higher concentrations of Cr, Co, Cu, Ti in the Mahi samples, but cannot simultaneously explain the depleted Sr in view of presence of Ca-rich phases (plagioclase + pyroxene) in the basalts. The decoupled behavior of Sr and Ca is thus interesting. In short, the Siwalik rocks may have had more mafic contributions than envisaged by Sinha et al. (2007), in addition to dominant granitoid contributions.

In this context, a plot of Mahi samples is closer to granodiorite in a Th–La–Sc diagram (Fig. 15a), but this does not necessarily justify a granodiorite source. The intermediate bulk compositions in the samples may be due to mixing between two end member compositions: the Deccan basalts and biotite-rich granitoid (alkali feldspar-free). A little variation of plagioclase contribution may have resulted in a range of negative Eu anomalies in the Mahi samples ($Eu/Eu^*$ 0.70–0.75), but still maintain Th/Sc ratios (0.3–0.4) similar to the source (about 0.3) (Fig. 15b). In the case of these rocks, increased contributions of Eu (plagioclase) and Sc (mafic minerals) yield higher $Eu/Eu^*$ than granitic source (0.72 vs. 0.60), and lower Th/Sc (about 1) in many samples, respectively. Reubi and Blundy (2009) have shown that mafic–felsic magma mixing/mingling is responsible for production of intermediate granodiorite magma in

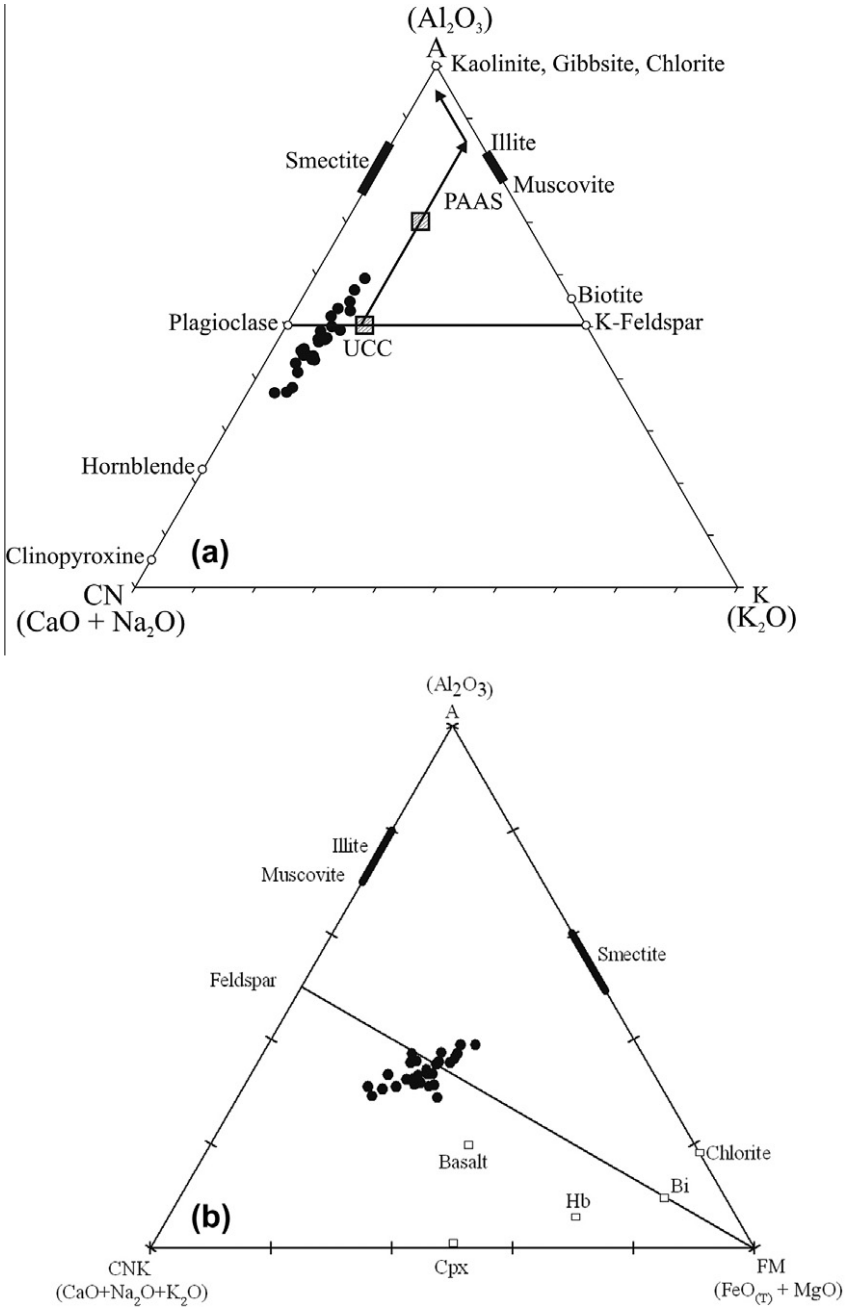


Fig. 12. Triangular (a) A–CN–K (b) A–CNK–FM plots of the Mujpur samples (for calculations of A, C, N, K, F and M components, see in text). (a) Samples plot at or about UCC; few samples plot even below upper continental crust (UCC: CIA = ~50) indicating presence of mafic components. (b) In A–CNK–FM plot, samples cluster halfway of feldspar–biotite join closer to field of basalt, consistent with presence of basalt fragments in the samples.

a subduction setting, instead of generation of a granodiorite melt equilibrated to a mantle source. Mixing between the two end-members (mafic and felsic sources) yielding intermediate bulk composition in sediments thus show remarkable commonalities indeed to Earth's magmatic processes.

### 5.5. Element mobility

In this section, the behavior of selected elements (K, Ba, Sr, Na, Ca and Mg), known to be mobile to extremely mobile during weathering, are addressed in the Mahi catchment and the Siwalik system. Because of the abundance of fine-sand/silt/clay, we assume that the Mahi alluvium and the Siwalik rocks represent bulk suspended load of their respective rivers. Interestingly, sediments in the Mahi and Siwaliks are depleted in these elements with respect to UCC (Fig. 14), and may have been lost as dissolved load.

Following Gaillardet et al. (1999), we define the mobility indices of an element by comparing its concentrations to that of an immobile element whose magmatic compatibility

Table 3
Geochemical mass balance calculation for the origin of Mujpur sediments and Siwalik siltstone/mudstone.

| | Tholeiitic basalt (Tho$^{\Phi}$) (avg. 10 samples) | Granitoids (BGC$^{\$}$) (avg. 5 samples) | 45% Tho | 50% Tho | 55% Tho | 65% Tho | 75% Tho | 85% Tho | Mujpur sediments (avg.)$^{\blacktriangle}$ | Siwaliks (avg.)$^{\#}$ |
|---|---|---|---|---|---|---|---|---|---|---|
| *Major element (wt. %)* | | | | | | | | | | |
| $SiO_2$ | 53.0 | 77.4 | 66.4 | 65.2 | 64.0 | 61.5 | 59.1 | 56.6 | 57.4 | 65.4 |
| $TiO_2$ | 1.46 | 0.25 | 0.80 | 0.86 | 0.92 | 1.04 | 1.16 | 1.28 | 1.65 | 0.73 |
| $Al_2O_3$ | 13.1 | 11.7 | 12.3 | 12.4 | 12.5 | 12.6 | 12.8 | 12.9 | 12.6 | 15.8 |
| $FeO^t$ | 13.6 | 0.85 | 6.59 | 7.23 | 7.86 | 9.14 | 10.4 | 11.7 | 7.69 | 5.88 |
| MnO | 0.21 | 0.02 | 0.11 | 0.12 | 0.13 | 0.15 | 0.16 | 0.18 | 0.11 | 0.06 |
| MgO | 6.29 | 0.52 | 3.12 | 3.41 | 3.69 | 4.27 | 4.85 | 5.42 | 2.27 | 2.59 |
| CaO | 7.81 | 0.93 | 4.03 | 4.37 | 4.71 | 5.40 | 6.09 | 6.78 | 5.04 | 1.60 |
| $Na_2O$ | 3.02 | 4.64 | 3.91 | 3.83 | 3.75 | 3.59 | 3.43 | 3.26 | 1.99 | 0.65 |
| $K_2O$ | 0.97 | 1.59 | 1.31 | 1.28 | 1.25 | 1.19 | 1.13 | 1.06 | 1.69 | 3.04 |
| $P_2O_5$ | 0.15 | 0.05 | 0.10 | 0.10 | 0.11 | 0.12 | 0.13 | 0.14 | 0.16 | 0.09 |
| *Trace elements (ppm)* | | | | | | | | | | |
| Cr | 256 | 4.20 | 118 | 130 | 143 | 168 | 193 | 218 | 294 | 150 |
| Ni | 98.8 | 2.03 | 45.6 | 50.4 | 55.3 | 64.9 | 74.6 | 84.3 | 38.5 | 57.7 |
| Sr | 169 | 81.0 | 120 | 125 | 129 | 138 | 147 | 155 | 183 | 87.1 |
| Rb | 30.4 | 27.8 | 29.0 | 29.1 | 29.2 | 29.5 | 29.8 | 30.0 | 68.4 | 140 |
| Ba | 251 | 265 | 259 | 258 | 257 | 256 | 255 | 253 | 192 | 474 |
| Th | 5.10 | 14.0 | 10.0 | 9.55 | 9.11 | 8.22 | 7.33 | 6.44 | 9.60 | 14.2 |
| Zr | 146 | 206 | 179 | 176 | 173 | 167 | 161 | 155 | 210 | 232 |
| La | 19.4 | 30.2 | 25.3 | 24.8 | 24.3 | 23.2 | 22.1 | 21.0 | 32.1 | 47.0 |
| Sm | 4.82 | 5.27 | 5.07 | 5.05 | 5.02 | 4.98 | 4.93 | 4.89 | 6.15 | 7.92 |
| Eu | 1.49 | 1.00 | 1.22 | 1.25 | 1.27 | 1.32 | 1.37 | 1.42 | 1.37 | 1.53 |
| Yb | 2.29 | 2.07 | 2.17 | 2.18 | 2.19 | 2.21 | 2.24 | 2.26 | 2.54 | 2.95 |

$^{\blacktriangle}$this work; $^{\#}$avg. 51 samples for major & trace elements and avg. 22 for REE (Sinha et al., 2007); $^{\Phi}$ and $^{\$}$: Ahmad and Tarney (1994).

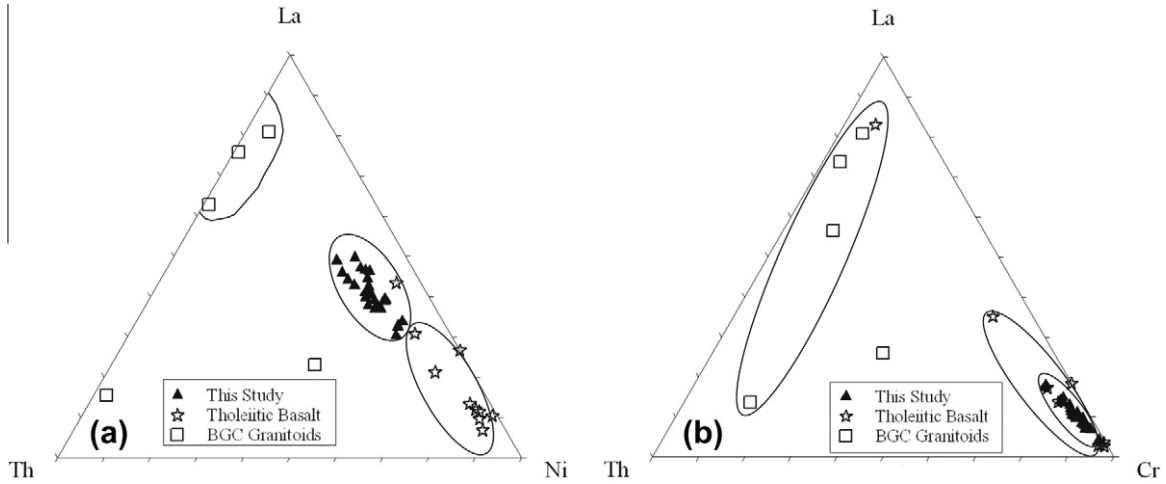


Fig. 13. (a) Th–La–Ni diagram showing samples plot towards La–Ni side, but clearly away from Th (felsic source), (b) Mujpur samples plot within the field of tholeiite basalt. Sources: Tholeiitic basalt and granitoid (Ahmad and Tarney, 1994).

is close to that of the given element. The mobility indices of an element are defind taking source rocks as Deccan LIP basalts of well known composition (Vijay Kumar et al., 2010) for the Mahi sediments, and UCC-type source for the Siwalik rocks (Sinha et al., 2007). The mobility indices ($\alpha_E$) for elements, as follows:

| For Mahi alluvium | For Siwalik rocks |
|---|---|
| $\alpha_K = [Th/K]_{mahi}/[Th/K]_{Deccan\ basalt}$ | $\alpha_K = [Th/K]_{siwa}/[Th/K]_{ucc}$ |
| $\alpha_{Ba} = [Th/Ba]_{mahi}/[Th/Ba]_{Deccan\ basalt}$ | $\alpha_{Ba} = [Th/Ba]_{siwa}/[Th/Ba]_{ucc}$ |
| $\alpha_{Sr} = [Nd/Sr]_{mahi}/[Nd/Sr]_{Deccan\ basalt}$ | $\alpha_{Sr} = [Nd/Sr]_{siwa}/[Nd/Sr]_{ucc}$ |
| $\alpha_{Na} = [Sm/Na]_{mahi}/[Sm/Na]_{Deccan\ basalt}$ | $\alpha_{Na} = [Sm/Na]_{siwa}/[Sm/Na]_{ucc}$ |
| $\alpha_{Ca} = [Ti/Ca]_{mahi}/[Ti/Ca]_{Deccan\ basalt}$ | $\alpha_{Ca} = [Ti/Ca]_{siwa}/[Ti/Ca]_{ucc}$ |
| $\alpha_{Mg} = [Al/Mg]_{mahi}/[Al/Mg]_{Deccan\ basalt}$ | $\alpha_{Mg} = [Al/Mg]_{siwa}/[Al/Mg]_{ucc}$ |

When there is no net chemical weathering, $\alpha_E = 1$. A value of >1 means a depletion with respect to source Deccan basalts (for Mahi samples), and the UCC (for Siwalik samples), and a value <1 means enrichment. The normalization to immobile elements removes the variations in absolute concentrations in suspended sediments, which may arise due to dilution by organic particulates or quartz. The quantitative results thus obtained are plotted in Fig. 16.

The order of decreasing mobility is Ba $\geqslant$ K > Ca (Fig. 16). The K, Ba, and Ca values show limited depletion in both the Mahi and Siwalik systems, although these samples have different weathering indices (CIA: 47.5 for Mahi vs. 69 for Siwaliks). The mobility of K, Ba, and Ca may therefore be climate insensitive. The more mobile behavior of Ba to Ca (known to be highly mobile) in the Mahi samples is surprising, as Ba is less mobile than Ca in Deccan Traps Rivers (see Das and Krishnaswami, 2006). Incipient weathering of pyroxene + plagioclase in the Mahi catchment perhaps causes Ca to be retained in the system. Alternatively, Ba may be more mobile in the Mahi than suggested for the Deccan Traps rivers, more similar to the Yamuna (Dalai et al., 2002) and Gomti Rivers (Munendra Singh, *pers. com.*) in northern India.

The behavior of Mg and Na, two known extremely mobile elements is still more interesting. In our samples, Mg is extremely depleted even in a weathering-limited condition. On the other hand, there is hardly any net gain or loss for Mg in the transport-limited Siwaliks. This may suggest insensitivity of Mg to climate too. Alternatively, the Mg behavior may be attributed to the enhanced contribution of an Mg-rich source (mafic) for the Siwaliks. The extreme Na mobility in the Siwalik sediments, unlike in the Mahi, is in agreement with general expectations. The Na-enrichment in our samples is likely due to interactions with sea water in estuarine conditions that might have adsorbed to the detritus.

Plagioclase may control both Ca and Sr distributions in the samples. The Pyroxenes and biotite, have Ca, but insignificant Sr ($Kd_{Sr} < 1$) (Hanson, 1978). Decoupled behavior

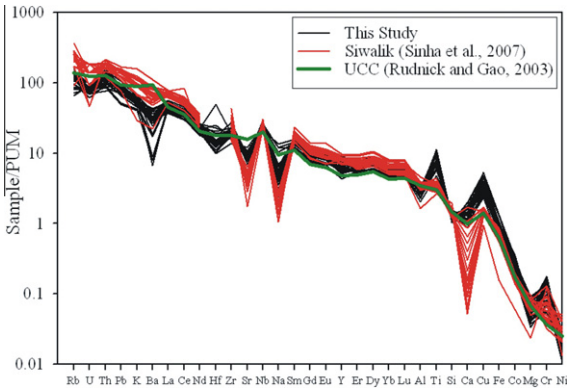


Fig. 14. Multi-element primitive upper mantle (PUM)-normalized pattern for the Mujpur and Siwalik samples. Note that the Siwalik siltstone are enriched in LIL and rare earth elements, but depleted in more compatible elements (Cr, Co, Cu) in comparison to the Mujpur alluvial samples. The negative anomalies of Ba, Sr, Na and Ca are characteristics of both plots (see text for details). Upper continental crust (UCC: Rudnick and Gao, 2003) is plotted for comparison. Composition of the Siwalik rocks from Sinha et al. (2007). PUM (primitive upper mantle) taken from Palme and O'Neill (2003).

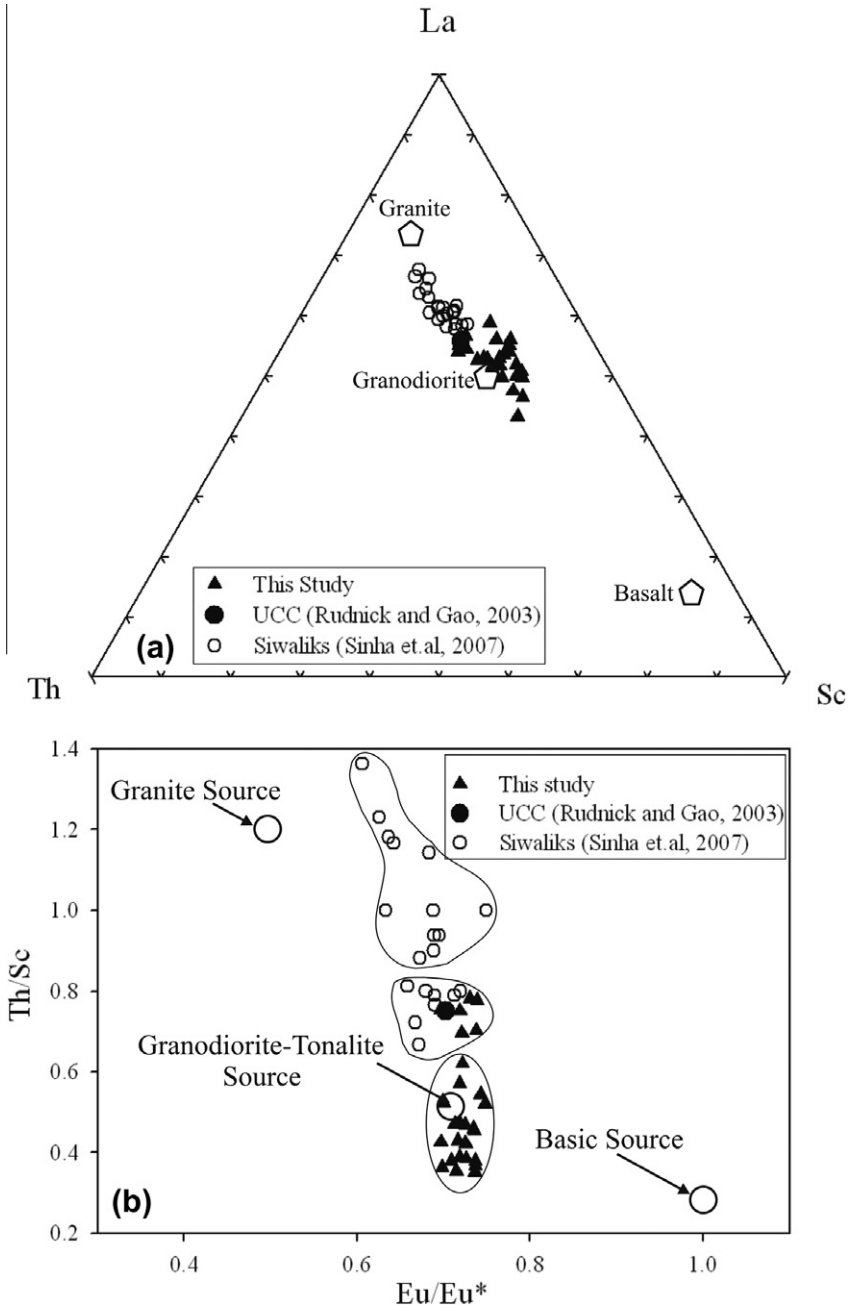


Fig. 15. (a) on Th–La–Sc diagram, Mujpur bulk samples plot closer to granodiorite. Intermediate compositions of the Mujpur samples attributable to mixing between the Deccan basalts and biotite-rich granitoid sources (see text). Spread of Siwalik rocks between granite and granodiorite compositions (closer to UCC) indicate dominant contributions of UCC-type sources. (b) On Th/Sc and Eu/Eu$^*$ diagram, Mujpur alluvium show more affinity to granodiorite-tonalite (more mafic) compared to UCC, whereas Siwalik rocks plot closer to UCC with few samples near granite source. Low Th/Sc (0.3–0.4) in Mujpur alluvium compared to the Siwalik rocks suggest more mafic contributions.

of Ca and Sr (see in Section 5.4) may therefore be related to pyroxene and biotite in the sources.

## 6. CONCLUDING REMARKS

(1) The Mahi sediments are lithiarenite and are composed of quartz + basalt fragments + pyroxene + biotite + feldspar + minor calcite + smectite + illite. These samples have $FeO^t$ ($\leqslant$10.9 wt.%), $TiO_2$ ($\leqslant$2.41 wt.%), $Al_2O_3$ ($\leqslant$15.16 wt.%), Cr ($\leqslant$737 ppm) higher than the UCC and PASS; Ni ($\leqslant$54 ppm) higher than the UCC (33.5 ppm), but close to PAAS (60 ppm). About 70–75% Deccan basalts and ~25–30% biotite-rich granitoid (Banded Gneissic Complex: BGC) mixture reasonably explain the composition of the bulk Mahi sediment.

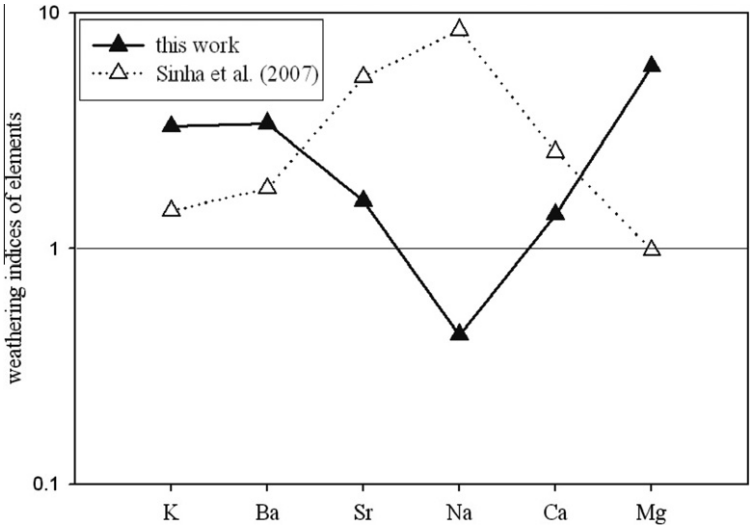


Fig. 16. Comparison of weathering indices of mobile K, Ba, Sr, Na, Ca, Mg in the Mahi catchment and Siwalik system. Note Ba and extremely mobile Ca show similar indices irrespective of chemical weathering. Ca and Sr show different mobility and decoupled. Mg is more mobile in the Mahi system.

(2) Mechanical processes, partly aided by winnowing of shallow sea water, controlled the texture in the Mahi sediments. Mineralogical and chemical characteristics of the sediments (except for Na) are not influenced by marine action and thus are representative of the catchments.
(3) The low CIA (37–59) and presence of basalt fragments and smectite suggest incipient or no chemical weathering in semi-arid condition. Tectonic-climatic condition promoted enhanced mechanical erosion, but inhibited chemical weathering in the production of the Mahi sediments.
(4) The Siwalik siltstone and mudstone may have more mafic contributions, in addition to dominant UCC-type source.
(5) The mobility of K, Ba, Ca are climate insensitive. More mobile behavior of Ba to Ca (known to be highly mobile) in the Mahi samples is new, as Ba is considered less mobile than Ca in Deccan Traps Rivers. The decoupled behavior of Ca and Sr, however, could be mineralogy controlled.
(6) Global continental provenance may not be of granodiorite compositions only. The discrepancies of Cr, Co and Cu in upper crustal compositions are better explained considering significant mafic contributions. Large igneous provinces (LIPs) may thus be important source globally in influencing upper crustal composition, in addition to understanding Earth's mantle.

## ACKNOWLEDGEMENTS

We thank the Director, BSIP, Lucknow for providing necessary help and support to carryout the work. Head of the Department of Geology, University of Lucknow and the Dean, Earth and Environmental Sciences, CUHP (Dharamshala) provided infrastructure during preparation of the manuscript. We also thank Directors of WIHG (Dehradun), IIT (Roorkee), and JNU (New Delhi) for extending analytical facility for data generation. AS and KK are grateful to Prof. L. S. Chamyal and his research group for extending logistic support during fieldwork. This work is greatly benefited from the incisive comments of official reviewers: Robert Cullers, Edward Tipper, Albert Galy and an anonymous reviewer. We also appreciate efficient handling of the paper by the Associate Editor Sydney Hemming. We also acknowledge Dr. Debajyoti Paul for reading and offering valuable suggestions for improving language and presentation of the manuscript. The present work is a part of the project (SR/S4/ES 21/Baroda Window/P1) of the Shallow Subsurface Study (SSS) program of Department of Science and Technology (DST), New Delhi. The financial support to KK in the form of a Fellowship by DST (Govt. of India) is gratefully acknowledged.

## REFERENCES

Abanda P. A. and Hennigan R. E. (2006) Effect of diagenesis on trace element partitioning in shales. *Chem. Geol.* **230**, 42–59.

Ahmad T. and Tarney J. (1994) Geochemistry and petrogenesis of late Archaean Aravalli volcanics, basement enclaves and granitoids, Rajasthan. *Precambrian Res.* **65**, 1–23.

Awwiller D. N. (1993) Illite/smectite formation and potassium mass transfer during burial diagenesis of mudrocks: a study from Texas Gulf coast palaeocene/eocene. *J. Sed. Petrol.* **63**, 501–512.

Basaltic Volcanism Study Project (BVSP), (1981) Pergamon Press, Inc., New York.

Basu A. (1985) Influence of climate and relief on composition of sands released at source areas. In *Provenance of Arenites: NATO ASI Series C: Mathematical and Physical Sciences*, vol. 148 (ed. G. G. Zuffa). D. Reidel Publishing Co., Dordrecht, pp. 1–18.

Biswas S. K. (1987) Regional tectonic framework, structure and evolution of western marginal basins of India. *Tectophysics* **135**, 307–327.

Bloch J. and Hutcheon I. E. (1992) Shale diagenesis: a case study from the Albian Hermon Member (Peace River Formation), western Canada. *Clays Clay Miner.* **40**, 682–699.

Bock B., McLennan S. M. and Hanson G. N. (1998) Geochemistry and provenance of the Middle Ordovician Austin Glen Member (Normanskill Formation) and the Taconian Orogeny in New England. *Sedimentology* **45**, 635–655.

Brantley S. L. (2003) Reaction kinetics of primary rock forming minerals under ambient conditions. Treatise on Geochemistry. ISBN (set): 0-08-043751-6, 5 (ISBN: 0-08-0044340-0). pp. 73–117.

Brügmann G. E., Arndt N. T., Hofmann A. W. and Tobschall H. J. (1987) Noble metal abundances in komatiite suites from Alexo, Ontario and Gorgona Island, Colombia. *Geochim. Cosmochim. Acta* **51**, 2159–2169.

Bryan S. E. and Ernst R. (2007) Revised definition of large igneous provinces (LIPs). *Earth Sci. Rev.* **86**(1–4), 175–202.

Chakraborty T. and Sensarma S. (2008) Shallow marine and coastal aeolian quartz arenite in the Neoarchaean-Palaeoproterozoic Karutola Formation, Dongargarh volcano-sedimentary succession, central India. *Precambrian Res.* **162**, 284–301.

Chamyal L. S., Maurya D. M. and Raj R. (2003) Fluvial system of dry lands of western India: a synthesis of late quaternary palaeoenvironmental and tectonic changes. *Quatern. Int.* **104**, 69–86.

Condie K. C. (1993) Chemical composition and evolution of the upper continental crust: contrasting results from surface samples and shales. *Chem. Geol.* **104**, 1–37.

Cox R. and Lowe D. (1995) A conceptual review of regional-scale controls on the composition of clastic sediment and the co-evolution of continental blocks and their sedimentary cover. *J. Sed. Res.* **65**, 1–12.

Dalai T. K., Krishnaswami S. and Sarin M. M. (2002) Major ion chemistry in the headwaters of the Yamuna River System: chemical weathering, its temperature dependence and $CO_2$ consumption in the Himalaya. *Geochim. Cosmochim. Acta* **66**, 3397–3416.

Das A. and Krishnaswami S. (2007) Elemental geochemistry of river sediments from the Deccan Traps, India: implications to sources of elements and their mobility during basalt–water interaction. *Chem. Geol.* **242**, 232–254.

Das A., Krishnaswami S., Sarin M. M. and Pande K. (2005) Chemical weathering in the Krishna Basin and Western Ghats of the Deccan Traps, India: rates of basalt weathering and their controls. *Geochim. Cosmochim. Acta* **69**, 2067–2084.

Das A. and Krishnaswami S. (2006) Barium in Deccan Basalt Rivers: its abundance, relative mobility and flux. *Aquat. Geochem.* **12**, 221–238.

Day P. R. (1965) Particle fractionation and particle-size analysis. In *Methods of Soil Analysis* (eds. C.A. Black, et al). *Agronomy* **9**, 545–577. Am. Soc. Agron. Inc., Madison, WI.

Dessert C., Dupre B., Francois L. M., Schott J., Gaillardet J., Chakrapani G. and Bajpai S. (2001) Erosion of Deccan Traps determined by river geochemistry: impact on the global climate and the 87Sr/86Sr ratio of sea water. *Earth Planet. Sci. Lett.* **188**, 459–474.

Dessert C., Dupre B., Gaillardet J., Francois L. M. and Allegre C. J. (2003) Basalt weathering laws and the impact of basalt weathering on the global carbon cycle. *Chem. Geol.* **20**, 1–17.

France-Lanord C. and Derry L. A. (1997) OC burial forcing of the carbon cycle from the Himalayan erosion. *Nature* **390**(9), 65–67.

Gaillardet J., Dupre B. and Allegre C. J. (1999) Global silicate weathering and $CO_2$ consumption rates deduced from the chemistry of large rivers. *Chem. Geol.* **159**, 3–30.

Galy A. and France-Lanord C. (2001) Higher erosion rates in the Himalaya: geochemical constraints on riverine fluxes. *Geology* **29**, 23–26.

Garver J. I., Royce P. R. and Smick T. A. (1996) Chromium and Nickel in shale of the Taconic foreland: a case study for the provenance of fine-grained sediments with an ultramafics source. *J. Sed. Res.* **100**, 100–106.

Gupta H. and Chakrapani G. J. (2005) Temporal and spatial variations in water flow and sediment load in Narmada River Basin, India: natural and man-made factors. *Environ. Geol.* **48**, 579–589.

Gupta H. and Chakrapani G. J. (2007) Temporal and spatial variations in water flow and sediment load in Narmada River Basin, India: natural and man-made factors. *Curr. Sci.* **92**(5), 679–684.

Gupta H., Chakrapani G. J., Kandasamy S. and Shuh-ji Kao. (2011) The fluvial geochemistry, contributions of silicate, carbonate and saline–alkaline components to chemical weathering flux and controlling parameters: Narmada River (Deccan Traps), India. *Geochim. Cosmochim. Acta* **75**, 800–824.

Hanson G. N. (1978) The application of trace elements to the petrogenesis of igneous rocks of granitic compositions. *Earth Planet. Sci. Lett.* **38**, 26–43.

Hessler A. M. and Lowe D. R. (2006) Weathering and sediment generation in the Archean: an integrated study of the evolution of the siliciclastic sedimentary rocks of the 3.2 Ga Moodies Group, Barberton Greenstone belt, South Africa. *Precambrian Res.* **151**, 185–210.

Jackson M. L. (1956) Soil Chemical Analysis – Advanced Course. Dept of Soils, Univ. of Wis., Madison 6, Wis. (Published by the Author).

Jackson M. L. (1973) *Soil Chemical Analysis*. Prentice Hall of India Pvt. Ltd., New Delhi.

Jaques A. L., Chappel B. W. and Taylor S. R. (1983) Geochemistry of cumulus peridotites and gabbros from the Marum Ophiolite Complex, northern Papua New Guinea. *Contrib. Mineral. Petrol.* **82**, 154–164.

Juyal N., Chamyal L. S., Bhandari S., Bhusan R. and Singhvi A. K. (2006) Continental records of southwest monsoon during the last 130 ka: evidence from the southern margin of the Thar Desert, India. *Quatern. Sci. Rev.* **25**, 2632–2650.

Khanna P. P., Saini N. K., Mukherjee P. K. and Purohit K. K. (2009) An appraisal of ICP-MS technique for determination of REEs: long term QC assessment of Silicate rock analysis. *Himalayan Geol.* **30**(1), 95–99.

Knuze G. W. (1965) Pre-treatment for mineralogical Analysis. In *Methods of Soil Analysis* (eds. C. A. Black, et al). *Agronomy* **9**, 568–577. Am. Soc. Agron., Madison, WI.

Krishnaswami S., Trivedi J. R., Sarin M. M., Ramesh R. and Sharma K. K. (1992) Strontium isotopes and Rubidium in the Ganga-Brahmaputra river system: Weathering in the Himalaya, fluxes to the Bay of Bengal and contributions to the evolution of oceanic $^{87}Sr/^{86}Sr$. *Earth Planet. Sci. Lett.* **109**, 243–253.

Kusumgar S., Rachna R., Chamyal L. S. and Yadav M. G. (1998) Holocene Palaeoenvironmental changes in the lower Mahi basin, western India. *Radiocarbon* **40**, 819–823.

Lee C.-T. A., Morton D. M., Little M. G., Kistler R., Horodysky U. N., Leeman W. P. and Agranier A. (2008) Regulating continental growth and composition by chemical weathering. *PNAS* **105**, 4981–4986.

Lupker M., France-Lanord C., Galy V., Lave J., Gaillardet J., Gajurel A. P., Cuilmette C., Rahman M., Singh S. K. and Sinha R. (2012) Predominant floodplain over mountain weathering of Himalayan sediments (Ganga basin). *Geochim. Cosmochim. Acta* **84**, 410–432.

Maurya D. M., Rachna R. and Chamyal L. S. (2000) History of tectonic evolution of Gujarat alluvial plains, Western India, during Quaternary: a review. *J. Geol. Soc. India* **55**, 343–363.

McDonough W. F. and Sun S.-s. (1995) The composition of the earth. *Chem. Geol.* **120**, 223–253.

McLennan S. M. (1989) Rare earth elements in sedimentary rocks: influence of provenance and sedimentary processes. In *Geochemistry and Mineralogy of Rare Earth Elements* (eds. B. R. Lipin and G. A. Mackay). Mineralogical Society of America, pp. 69–200.

McLennan S. M. (2001) Relationships between the trace element composition of sedimentary rocks and upper continental crust. *Geochem. Geophys. Geosys.* **2**, 2000GC00109.

McLennan S. M. (2003) Sedimentary silica on Mars. *Geology* **31**, 315–318.

Merh S. S. (1995) Geology of Gujarat. *J. Geol. Soc. India*, 222p.

Nesbitt H. W. and Young G. M. (1984) Prediction of some weathering trends of plutonic and volcanic rocks based on thermodynamic and kinetic considerations. *Geochim. Cosmochim. Acta* **54**, 1523–1534.

Nesbitt H. W. and Young G. M. (1989) Formation and diagenesis of weathering profiles. *J. Geol.* **97**, 129–147.

Palme H. and O'Neill H. St. C. (2003) Cosmochemical estimates of mantle composition. Treatise on Geochemistry. ISBN (set): 0-08-043751-6, 2 (ISBN: 0-08-044337-0). pp. 1–38.

Pettijohn F. J., Potter P. E. and Siever R. (1972) *Sand and Sandstones*. Springer-Verlag, New York.

Piper D. Z. (1974) Rare Earth elements in the sedimentary cycles: a summary. *Chem. Geol.* **14**, 285–304.

Purohit K. K., Saini N. K. and Khanna P. P. (2010) Geochimical dispersion pattern of heavy metal abundances in the intermontane Pinjaur Dun, Sub-Himalaya. *Himalayan Geol.* **31**(1), 29–34.

Rachna R., Maurya D. M. and Chamyal L. S. (1999) Tectonic control on distribution and evolution of Ravines in the lower Mahi valley, Western India. *J. Geol. Soc. India* **52**, 669–674.

Reubi O. and Blundy J. (2009) A dearth of intermediate melts at subduction zone volcanoes and the petrogenesis of arc andesites. *Nature* **461**, 1269–1273.

Rudnick R. L. (1995) Making continental crust. *Nature* **378**, 571–578.

Rudnick R. L. and Gao S. (2003) Composition of the continental crust. Treatise on Geochemistry. ISBN (set): 0-08-043751-6, 3 (ISBN: 0-08-0044338-9). pp. 1–64.

Saini N. K., Mukherjee P. K., Rathi M. S. and Khanna P. P. (2000) Evaluation of energy dispersive X-ray fluorescence spectrometry in the analysis of silicate rocks using pressed powder pellets. *X-Ray Spectrom.* **29**, 166–172.

Sarin M. M., Krishnaswami S., Dilli K., Somayajulu B. L. K. and Moore W. S. (1989) Major ion chemistry of the Ganga–Brahmaputra river system: weathering processes and fluxes to the Bay of Bengal. *Geochim. Cosmochim. Acta* **53**, 997–1009.

Sensarma S. (2007) A bimodal large igneous province and the plume debate: the Palaeoproterozoic Dongargarh Group, Central India. *Geol. Soc. Am. Spec. Pap.* **430**, 831–839.

Sensarma S., Rajamani V. and Tripathi J. K. (2008) Petrography and geochemical characteristics of the sediments of the small River Hemavati, Southern India: implication for provenance and weathering processes. *Sed. Geol.* **205**, 111–125.

Shapiro L. and Brannock W. W. (1962) Rapid analysis of silicate, carbonate and phosphate rocks. *US Geol. Surv. Bull.* **48**, 49–55.

Sharma A. and Rajamani V. (2001) Weathering of charnockite and sediment production in the catchment area of the Cauvery River, southern India. *Sed. Geol.* **143**, 169–184.

Sharma A., Singh A. and Kumar K. (2012) Environmental geochemistry and quality assessment of surface and subsurface water of Mahi River basin, western India. *J. Environ. Earth Sci.* **65**(4), 1231–1250.

Sharma S. K. and Subramanian V. (2008) Hydrochemistry of the Narmada and Tapti Rivers, India. *Hydrol. Process.* **22**, 3444–3455.

Sheth H. C. (2007) Large igneous provinces (LIPs): definition, recommended terminology, and a hierarchical classification. *Earth Sci. Rev.* **85**(3–4), 117–124.

Singh P. and Rajamani V. (2001) REE geochemistry of recent clastic sediments from the Cauveri floodplain, southern India: implication to source area weathering and sedimentary processes. *Geochim. Cosmochim. Acta* **65**, 3093–3108.

Singh S. K., Kumar A. and France-Lanord C. (2006) Sr and $^{87}Sr/^{86}Sr$ in waters and sediments of the Brahmaputra river system: silicate weathering, $CO_2$ consumption and Sr flux. *Chem. Geol.* **234**, 308–320.

Singh S. K., Rai S. K. and Krishnaswami S. (2008) Sr and Nd isotopes in river sediments from the Ganga Basin: sediment provenance and spatial variability in physical erosion. *J. Geophys. Res.* **113**, F03006. http://dx.doi.org/10.1029/2007JF000909.

Sinha S., Islam R., Ghosh S. K., Kumar Rohta and Sangode S. J. (2007) Geochemistry of Neogene Siwalik mudstone along Punjab re-entrant, India: implication for source-area weathering, provenance and tectonic setting. *Curr. Sci.* **92**(8), 1103–1113.

Stallard R. F. and Edmond J. M. (1983) Geochemistry of the Amazon: 2. The influence of geology and weathering environment on dissolved load. *J. Geophys. Res.* **88**, 9671–9688.

Stork A. L., Smith D. K. and Gill J. B. (1987) Evaluation of geochemical reference standards by X-ray fluorescence analysis. *Geostand. Newslett.* **11**, 107–113.

Suttner L. J. (1974) Sedimentary petrographic provinces: an evaluation. In *Paleogeographic Provinces and Provinciality* (ed. C. A. Ross). *SEPM Spec. Publ.* **21**, 75–84.

Tandon S. K., Jain M. and Singhvi A. K. (1999) Comparative development of mid to late quaternary fluvial and Fluvio–aeolian stratigraphy in the Luni, Sabarmati and Mahi river basin of western India. *Gond. Geol. Mag. Spec. Vol.* **4**, 1–16.

Tanner C. B. and Jackson M. L. (1947) Monographs of sedimentation times for soil particles under gravity or centrifugal acceleration. *Proc. Soil. Sci. Soc. Am.* **12**, 50–55.

Taylor S. R. and McLennan S. M. (1985) *The continental crust: its composition and evolution*. Blackwell, Malden, MA, 312 pp.

Vijay Kumar K., Chavan C., Sawant S., Naga Raju. K., Kanakdande P., Patode S., Deshpande K., Krishnamacharyulu S. K. G., Vaideswaran T. and Balaram V. (2010) Geochemical investigation of a semi-continuous extrusive basaltic section from the Deccan Volcanic Province, India: implications for the mantle and magma chamber processes. *Contrib. Mineral. Petrol.* **159**, 839–862.

Whitmore G. P., Crook K. A. W. and Johnson D. (2004) Grain size control of mineralogy and geochemistry in modern river sediment, New Guinea collision, Papua New Guinea. *Sed. Geol.* **171**, 129–157.

*Associate editor*: Sidney Hemming